INVESTIGATION OF FIBER REINFORCED FERROCEMENT COMPOSITES IN RETROFITTING REINFORCED CONCRETE BEAMS

By

ELIE I HADDAD

A thesis submitted to the

School of Graduate Studies

Rutgers, The State University of New Jersey

In partial fulfillment of the requirements

For the degree of

Master of Science

Graduate Program in Civil & Environmental Engineering

Written under the direction of

Hani H. Nassif

And approved by

_____

_____

_____

_____

New Brunswick, New Jersey

October, 2018

ABSTRACT OF THE THESIS

Investigation of fiber reinforced ferrocement composites in retrofitting reinforced concrete beams

By ELIE I HADDAD

Thesis Director:

Hani H. Nassif

Reinforced concrete bridge decks tend to deteriorate over time due to the increase in live load and corrosion of reinforcement and many other reasons. Economic factors do not allow for a complete replacement of such structures which validates the importance of concrete rehabilitation technologies. With the launch of high performance materials, the use of cementitious composites for infrastructure application for rehabilitation has become more common. Ferrocement application for bridge decks repairs is inexpensive and can extend the life of the bridge by 5 to 10 years.

This study presents the results of an experimental research performed to investigate the behavior of damaged reinforced concrete beams repaired with fiber reinforced ferrocement laminate. The ferrocement layer acts as a replacement to a damaged or peeled off clear cover. A total of 30 beams were tested under two point loading system up to failure. The research work discusses the effect of; the number and type of reinforcement in the laminate, and the incorporation of macro polypropylene fibers at different volume in the mortar used for the repair layer. The beams differed by their reinforcement ratios in the ferrocement laminate, thickness of the lamniate, size and

number of shear studs which act as a bond between the two layers. All beams are designed to fail in flexure.

Results showed that the beams tested had noticeable improvement in terms of ductility, cracking strength (163%) and ultimate capacity (109%). The results also showed the material properties of multiple mortar mixes that were considered to be used for the fabrication of the repair layers. These mixes differed by their cementitious components, fibers content, and other parameters that will be discussed later on are in the study.

ACKNOWLEDGEMENTS

I would like to thank Dr. Hao Wang and Dr. Abu Obeidah for being on my committee.

I would also like to thank all the undergraduate research assistants, Alain, Albert, Andrew, Dan, Emily, that helped with mixing and preparing beams to accomplish this study, as well as Mirelle for her help crack mapping.

I would like to thank Dr. Abu-Obeidah for the guidance he has provided me over the past few years, as well as graduate students, Jon Rodriguez, Chris Sholy and Greg Brewer.

I would like to thank the RE-CAST University Transportation Center for funding my research, as well as the Rutgers Civil & Environmental Engineering department.

Most importantly, I want to deeply thank Dr. Hani Nassif for investing in me, giving me the opportunity of working in his research group. Dr. Nassif gave me the chance to prove myself as an undergraduate research assistant which I am very grateful for. It has been an honor working with him.

TABLE OF CONTENT

LIST OF TABLES

LIST OF FIGURES

CHAPTER I

1 INTRODUCTION

1.1 PROBLEM STATEMENT

According to the Federal Highway Administration (FHWA), many bridges in the United States are in desperate need of maintenance due to many factors. The number of deficient bridges is on the rise mainly due to bridge deterioration and increasing live load. This shows that 8.9% of the nation's bridges are structurally deficient. (Federal Highway Administration, FHWA 2016).

There are many factors that cause bridges to deteriorate such as cracking and spalling of concrete, environmental conditions like corrosion, and extremely heavy truck loads (Nassif & Najm, 2005). According to Nassif and Najm (2005), deck delamination and concrete spalling are the most common types of bridge deterioration. In such a case concrete cover becomes loose and could peel off, exposing the reinforcement steel bars to the outside environment causing damage to the structure. Deicing salts aggravates the problem of concrete spalling because of its ability to corrode steel. Furthermore, concrete decks suffering from delamniation or spalling experience high live load, they detriorate at a higher rate.

Ferrocement layer replaces the clear cover that was peeled off due to overuse and when maintenance is urgently needed. The use of ferrocement layer as a repair technique

increases the capacity of the bottom fibers resulting in an increase in its tensile strength and modulus of rupture. Thus, improving the tensile strength of decks which will result in less susceptibility to corrosion, higher cracking capacity, and better fatigue performance (Nassif & Najm, 2004).

This paper investigates the performance of such composites under static flexural loading as well as the effect of; the number of mesh in the laminate, different bonding and reinforcement systems, and incorporation of polypropylene fibers in the repair layer.

1.2 RESEARCH OBJECTIVES AND SCOPE

The purpose of this study is to investigate the behavior of reinforced concrete beams retrofitted with fiber reinforced ferrocement laminates. Multiple mortar mixes have been investigated in order to determine the optimum mix to be used for the study, their mechanical properties have been collected and reported. Reinforced concrete beams with a peeled off clear cover are repaired with a fiber reinforced ferrocement laminate. Thirty beams including five control beams and twenty five retrofitted ones are tested until failure under three-point flexural loading system. This study shows the behavior of these beams in terms of deflection, ductility, cracking, and ultimate capacity. These beams differ by the thickness of their ferrocement layer ranging from 1 to 1.5 inch, the mix used in the preparation of the laminate, the number of mesh in the laminate, amount of fibers in the laminate, and by the number and size of stirrups in the substrate that also acts as a bond between the two layers.

1.3 THESIS ORGANIZATION

This thesis consists of five chapters as the following:

Chapter I serves as an introduction consisting of the problem statement, research objective and scope and thesis organization.

Chapter II covers the general background and literature review on the type of detrioration of bridge decks, different repair materials, definition of ferrocement, past research on fiber reinforced ferrocement and beam repairs.

Chapter III covers the experimental program including the material properties and supplies, mix designs and the mixing and testing procedures.

Chapter IV covers the results of the tests, including the mechanical properties of the mortar mixes as well as their free shrinkage results, and the beam testing results.

Chapter V covers the conclusions, recommendations and possible scope for future research.

CHAPTER II

2 LITERATURE REVIEW

2.1 INTRODUCTION

Sustainable infrastructures are those that need the least intervention during their lifetime and that why they are crucial for economic development (Safdar et al., 2016). According to Bruhwiler and Denarie (2013), reinforced concrete structures show noticeable poor performance in terms of structural behavior and durability under severe environmental conditions and high mechanical loading.

Nassif and Najm (2004) stated that the main causes of deterioration of concrete bridge decks are: (1) cracking and spalling of concrete (2) environmental conditions such as corrosion, and (3) extremely heavy truck loads. The most common types of deterioration are deck delamination and concrete spalling. In such cases, the concrete clear cover loosens and could peel off. The steel reinforcement then gets exposed to the external environment, which in terms harms the structure. Furthermore, the spread of deicing salts during snow periods aggrevates the problem of concrete spalling. Additionally, trucks that exceed the weight limit would cause delaminated or spallen concrete decks to weaken even more (Nassif & Najm, 2004). Nowak et al. (1994) studied the effect of truck loading on bridges. In this study, data on truck weight was gathered (over 600,000-truck record) from Weigh Stations, Weigh-In- Motion measurements, and overweight trucks from the Motor Carrier Division of the Michigan State Police. It was

shown that numerous trucks exceeded the State legal limits on truck gross weight, which in terms would shorten the life expectancy of such structures. According to Nassif and Najm (2004), the frequent passage of heavy trucks results in large stress ranges at a large number of cycles causing a shorter fatigue life. Therefore, there is a need to control cracking of bridge decks.

2.2 DETERIORATION OF CONCRETE

2.2.1 Cracking and Spaling of Concrete

According to ACI Committee 116R (2000), concrete deck delamination usually occurs as a result of separation in the concrete layers parallel and close to the surface, at or close to the outermost layer of the rebar. When corrosion induced cracks join together to form a fracture plane, the separation of the concrete layers takes place (Gheitasi and Harris, 2015). Since delamination is characterized by a random and irregular pattern, it is historically considered as one of the most complicated issues associated with in-service concrete structures (Gheitasi and Harris, 2015). The location and degree of level of concrete deck delamination depend on the environmental condition, which in turn directly influences the corrosion rate, and also depends on the geometrical configuration of the concrete member such as cover thickness, rebar diameter and spacing (Gheitasi and Harris, 2015). Furthermore, spalling is the deterioration mechanism that occurs once the delaminated area reaches the surface and completely separates from the concrete member (Gheitasi and Harris, 2015). According to FHWA (2012), delamination and spalling can happen on both the top surface and bottom of an operating reinforced concrete slab. While these deterioration mechanisms may not lead to a structural failure or collapse, in

most cases they can cause a major impact on the serviceability and functionality, in addition to disfiguring the appearance of the structure (Gheitasi and Harris, 2015).

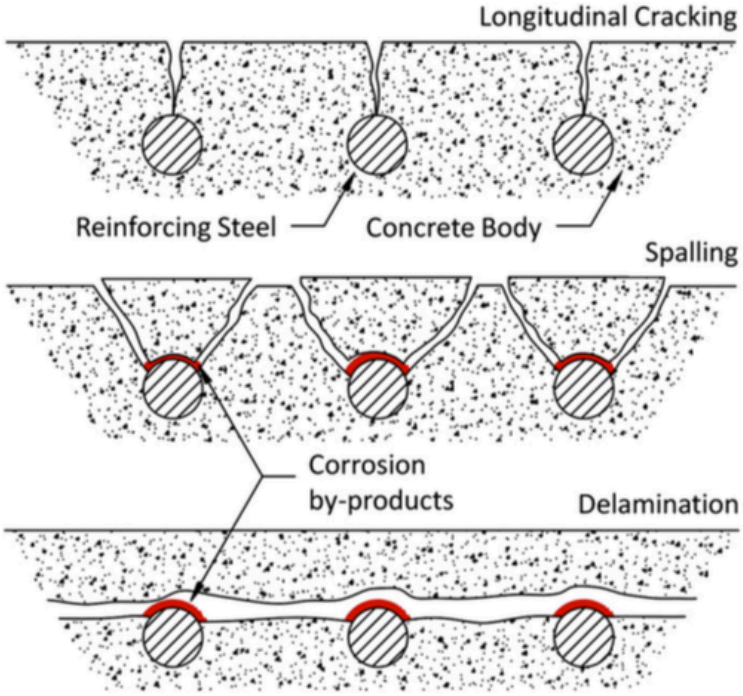

Figure 2. 1: Corrosion-induced damage scenarios

Reprinted from "Performance assesment of steel-concrete composite bridges with dubsurface deck deterioration" by A. Gheitasi, D.K. Harris, 2014, The institution of Structural engineers, 2353-0124

2.2.2 Corrosion of Reinforcement

In reinforced concrete structures, it is known that the reinforcing steel is necessary to maintain the strength of the structure; however, corrosion is a major concern. According to NASA, Kennedy Space Center, Corrosion Technology Laboratory (n.d.), there are two theories on how corrosion in reinforced concrete can occur,

1- Salts and other chemicals enter the concrete and cause corrosion of the reinforcing steel which in turns leads to an expansion of the metal leading to cracks in the concrete.

2- when reinforced concrete members crack, moisture and salts can reach the surface of the reinforcing bars and also leading to corrosion.

Adequate depth of cover can lower the chances of corrosion in concrete by embedding the steel deep enough to prevent chemicals from the surface from reaching the steel. Other methods of protecting reinforcement and reducing corrosion rate would be to maintain the water/cement ratio below 0.4, having a high cement factor, proper detailing to prevent cracking and ponding, and the use of chemical admixtures. Although these methods are effective, unfortunately, many concrete structures do corrode. When this occurs, remedial action is required, repairing the cracked and spalled concrete, coating the surface to prevent further entry of corrosive chemicals into the structure, or cathodic protection, an electrical means of corrosion control.

When steel rebars in reinforced concrete corrode, deflection and cracking width increase under service load, while ultimate strength decreases (Rodriguez et al. 1997). In addition, Rodriguez et al. (1996) showed that a corrosion degree of 14% leads to a decrease in strength of 23% for the beam. Misra and Uomoto (1987) reported that 2.4% corrosion caused a 17% reduction in beam strength. Furthermore, the ductility of reinforced concrete is also highly affected by reduction in the cross-sectional area of the steel reinforcement. Cairns et al. (2005) showed that a reinforcement bar with an 8% reduction in cross-section, suffered approximately from a 20% loss of its original ductility. Consequently, there is a need to control corrosion.

2.2.3 Overweight trucks

Overweight trucks can accelerate the deterioration process of concrete decks that

suffer from delamination or spalling. Nowak et al. (1993) showed that many trucks exceeded the State legal limits on truck gross weight by gathering data on truck weight (over 600,000-truck record) from Weigh Stations, Weigh-In- Motion measurements, and overweight trucks from the Motor Carrier Division of the Michigan State Police. Heavy load vehicles can significantly reduce the life of a structure. In addition, the recurring passage of heavy trucks leading to a wide stress ranges at a high number of cycles, meaning a shorter fatigue life (Nassif & Najm, 2004). Hence, there is a need to control cracking of bridge decks.

2.3 REPAIR TECHNIQUES

As discussed in the previous section, reinforced concrete structures tend to deteriorate for multiple reasons and there is a need for cost effective repair method and design in order to extend the life of such damaged structures.

2.3.1 Fiber Reinforced Polymer Sheets

A widely used technique to strengthen and rehabilitate reinforced concrete structural members in flexure and shear is the addition of an externally bonded fiber reinforced polymer (FRP) laminates (Hawileh et al., 2013). Accodring to Hawileh et al. (2013), some of the benefits of using FRP composites are; high strength-to-weight ratio, resistance to corrosion and high durability. Glass, carbon, or hybrid FRP are being implemented in different shapes such as sheets, strips, grids, rods and tendons, with different adhesive for reinforcing structural members like slabs, beams and columns (Hawileh et al., 2013). Research has shown a remarkable increase in load carrying capacity for members strengthened with FRP materials at controlled temperatures

(Hawileh et al., 2013). Furthermore, the use of a hybrid combination of carbon and glass FRP sheets in strengthening reinforced concrete beams and slabs in flexure has shown to improve the strength and ductility. However, Hawileh et al. (2013) showed that FRP laminates tend to loose a significant percentage of their modulus of elasticity and their tensile strengths when exposed to high temperature. FRP specimens fail in a brittle mode by rupture of the fiber (Hawileh et al., 2013).

2.3.2 External Post Tensioning using steel tendons

Another method of beam repairs is the external post tensioning using steel tendons. However, the corrosion of steel due to its exposure to the outside environment is a major setback. Instead, the use of fiber reinforced polymer could be a better alternative to steel, but its anchorage is complicated (Abu Obeidah, 2017).

2.4 FERROCEMENT

2.4.1 Definition of Ferrocement

According to ACI committee 549 (1997), ferrocement is a type of reinforced concrete that mainly differs from standard reinforced concrete by the dispersion and arragement of the reinforcement. Ferrocement contains mesh layers or rods, closely spaced, fully embedded in cement mortar. It is not the same as conventional reinforced concrete because it performs differently in terms of strength, deformation and potential application. Ferrocement can be shaped into very thin sections. The reinforcement used in its formation can be assembled into the desired final shape of the ferrocement, before the mortar can be coated directly in place. In such cases, forms are not needed, which is one of the benefits of ferrocement.

Ferrocement is defined by the mixture of a ferrous reinforcement implanted in a cementitious substance (ACI Committee 549, 1997). However, reinforcement types are not limited to steel meshes or rods. For example, the ancient and general method of building single story buildings by using reeds to reinforce dried mud could be considered a predecessor of ferrocement (ACI Committee 549, 1997). Futhermore, The use of non-metallic mesh such as woven alkali resistant glass, organic woven fabrics such as polypropylene, and organic natural fabrics made with jute, burlap, or bamboo fibers are being explored around the world (ACI Committee 549, 1997). Thus, the term ferrocement currently does not imply the use of ferrous materials. The definition that ACI committee 549 (1997) adopted: "*Ferrocement is a type of thin wall reinforced concrete commonly constructed of hydraulic cement mortar reinforced with closely spaced layers of continuous and relatively small size wire mesh. The mesh may be made of metallic or other suitable materials."* The definition indicates that, since ferrocement is a form of reinforced concrete, it is a composite material, therefore the basic concepts that describe the behavior and mechanics of composite materials should be also applicable to ferrocement (ACI 549, 1997). According to Makki (2014), Ferrocement is characeterised by its degree of toughness, ductility, durability, strength and crack resistance, qualities that are signigicantly greater than those found in other forms of concrete construction. These attributes are achieved in the structures with a thickness that is usually less than 25 mm, a dimension that is unlikely to be found in other construction materials, and a clear advancement compared to conventional reinforced concrete (Makki, 2014). For these reasons, ferrocement can be considered a high technology material (Makki, 2014).

Mortar is brittle, however, when it is reinforced with ductile wire mesh, ferrocement acts as a composite material (Makki, 2014). The presence of closely distributed wires with small spacing, in the rich cement sand mortar, transmit ductility and improve crack resistance mechanism (Makki, 2014).

It is also important to note that due to the small thickness of this material, the self weight of ferrocement elements per unit area is relatively smaller to reinforced concrete elements. Ferrocement can be 10 mm thin while the minimum thickness for reinforced concrete shells or plates is around 75 mm (Makki, 2014). Due to its low self weight as well as high tensile strength ferrocement is considered a favourable material for fabrication. With small diameter wire mesh reinforcement distributed over the entire surface, the material obtains a high resistance to cracking, an improved degree of toughness, fatigue resistance, and impermeability. With regards to Makki, (2014), the most notable differences between conventional reinforced concrete and ferrocement are:

1. Ferrocement can be formed in much thinner sections
2. Ferrocement mix proportions mainly consists of Portland cement while regular concrete consist of coarse aggregate
3. The reinforcement in the ferrocement is made of a large amount of smaller diameter wire meshes instead of reinforcing bars in reinforced concrete.
4. Ferrocement has a greater percentage of reinforcement, distributed throughout the section.
5. The structural behavior of ferrocement: high tensile strength and superior cracking performance.
6. with regard to construction, formwork is rarely needed.

2.4.2 Fiber Reinforced Ferrocement

Mosavi (2017), evaluated the effect of partially replacing cement with silica fume (SF) on the flexural strength and cracking development of simply supported ferrocement panels, reinforced with steel fiber and wire mesh. In his study, different dosages of silica fume and steel fiber were mixed and compared with a reference mortar mix. The panels also included 1, 2 and 3 layers of galvanized wire mesh. Mosavi (2017) studied the 28-day flexural strength of these panels by performing center point flexural tests. Flexural performance was evaluated by stress deflection results of the panels. Number of cracks developed at failure, average crack width and crack spacing were also taken into account. Mosavi (2017) found that 15% cement replacement with silica fume in addition to 4% of steel fiber addition in the mortar mix resulted in a 360% increase in flexural strength at 28 days compared to reference standard mortar. Therefore, the inclusion of 4% steel fibers in a mortar of fabricated ferrocement panels improved the crack resistance and flexural capacity. Mosavi (2017), found that the optimal panel included 15% SF, 4% Steel fibers, and 3 layers of wire mesh. The study also showed that the flexural strength and mid span deflection increased when the number of galvanized wire mesh increased. Mosavi (2017) also concluded that the crack width of the ferrocement panels decreased when the number of wire mesh increased.

2.5 FERROCEMENT APPLICATION FOR REPAIRS AND REHABILITATION

Makki (2014), studied the behavior of reinforced concrete beams retrofitted by ferrocement in terms of shear and flexural capacity. Some beam specimens were

strengthened and others were repaired. Repaired beams are loaded to 50% or 70% of their ultimate strength before being retrofitted. The parameters studied are the effect of different types of shear reinforcement, and the effect of the diameter of the wire mesh (1.2 or 2.2 mm). The mechanical methods of attaching the ferrocement layer to the reinforced concrete beam using bolts is also evaluated in this study. Retrofitting occurred by drilling holes on both sides of the beam specimens, then mesh is wrapped around the 3 sides (left, bottom and right) and bolts are used to fix the wire mesh. Then the mortar layer is casted on the 3 sides that are wrapped with the mesh. This approach was used in order to minimize chances of substrate and laminate debonding. the results of this study showed an increase in ultimate load (69.8-175% for strengthening) and (50.94-125% for repairing) when compared with control beams. for the strengthened beams, the diameter of ferrocement wire mesh (changing from 1.2 to 2.2mm) caused an increase ranging from 95% to 175% on the ultimate load for beams without steel stirrups and a 69.8%-126.4% for beams with stirrups steel. For the repaired beams, changing from 1.2 to 2.2mm diameter wire mesh, increased the ultimate strength of R.C. beams by 67.5-125% for specimens without steel stirrups and (50.94-84.9% for specimens with steel stirrups. Additionally, Makki (2014) concluded that the use of ferrocement meshes as external strengthening or repairing technique, delayed the crack appearance and reduced the crack width, while also showing large deflection at the ultimate load. Both strengthened and repaired beams experienced the same behavior with the ferrocement system, however the strengthened beams had a higher percentage increase in ultimate load than that of repaired beams of same conditions. Failure of these beams occurred by the development of shear and flexural cracks over the tension zone. However, the crack spacing is smaller

when large wiremesh was used in the ferrocement laminate causing a better stress distribution when compared to beams that had small wiremesh.

Khan et al. (2013), evaluated the effectiveness of ferrocement strengthening techniques by casting in situ as well as precast laminate. For the purpose of this study, ten reinforced concrete beams including one control beam, designed to fail in flexure, were cast and loaded under a third point loading system until service limit. After loading, beams were strengthened in the flexural dominant region only and tested again until failure. Their results showed that cast in situ ferro mesh layer is more effective than using precast layers. They also concluded that the use of 3 mesh layers increased the load carrying capacity and stiffness of the the repaired beams when compared to 2 mesh layers, however, ductility did not differ much for beams that had 2 or 3 layers of mesh.

Nassif and Najm (2003) studied the composite behavior of reinforced concrete beams overlaid on a thin section of ferrocement. Particularly, the method of shear transfer between the two layers was examined. A variety of beams with different mesh types, hexagonal and square, were tested to failure under a two point loading system. dimensions were reduced geometrically from an actual bridge deck. Beams were cast in scaled dimensions of the actual bridge deck slabs between two adjacent girders. All beams are designed to be minimally-reinforced. All beams in the study were of dimensions of 6”x6”x40” with an effective length of 36”, and had a #3 rebar as the main reinforcement in the concrete layer located at a depth of 4.5”. The shear studs used were (No. 3) reinforcement. The mix design used for mortar was performed according to the guidelines of ACI Committee 549 (1997)for design and construction of ferrocement. The study presented the analysical and experimental results. The beam were cast in two

groups. The first group (A) included a total of eight beams, with two control beams, and 6 identical beam that only differed by the the number of mesh in the laminate and the mesh type (2, 4, 6, hexagonal or square). Group A beams, had five shear studs, or hooks, (U shaped) spaced equally along the beam. The second group of beams had different types of shear studs. The purpose was to study the composite behavior of both layers and the required number of studs that would cause flexural failure instead of bond type of failure. The volume fraction of the reinforcement for both sets were within the provisions given in the ACI Committee 549 guidelines (Section 4.5), which requires the total volume fraction for non-prestressed water retaining structures to be a minimum of 3.5%. beam were tested after 28 days of curing at room temperature under 100% humidity. Nassif and Najm (2004) concluded that a minimum number of five studs is needed to provide full composite action between both layers. Beams having shear studs with hooks (U shaped) demonstrated better pre-cracking stiffness as well as cracking strength compared to beams with L-shaped studs. Their results also showed that beam specimens with square mesh had better cracking capacity than the control beam as well as beams with hexagonal mesh. Yet, the change in the ultimate capacity was not significant. In addition, the finite element model done in this study showed accurate prediction of ultimate moment capacity for beam that included the required number of shear connectors for full composite action.

CHAPTER III

3 EXPERIMENTAL SETUP

3.1 INTRODUCTION

The experimental work performed for this study included different mortar mixes varying by their cementitious materials, different fiber types, and the chemical admixtures that were used. These mortar mixes are studied and evaluated in order to find the optimal mixes to be used for the preparation of the ferrocement layer. Two different mixes were used for the preparation of the repair layer of the beams.

30 simple beams, designed to fail in flexure, were prepared and tested under a third-point flexural loading system. The beams were spread into five groups. Molds were prepared, shear reinforcement was fixed, class A base mix was cast. Afterwards, the mesh was put in place, and on the 21st day after the base mix was cast, mortar mix was cast. Seven days later, beams were tested. Beam Testing occurred on the 28th day after the class A base mix was casted and seven days after the ferrocement layer was placed.

3.2 MATERIAL PROPERTIES

Materials used for the fabrication of the substrate and laminate are obtained from various suppliers. Aggregates, both fine and coarse, as well as Portland Cement, are obtained from Claytom Concrete in Edison, New Jersey. Chemical admixtures such as water reducer, air entrainer, and crack reducer are provided by Master Builders. Fibers

are obtained from Euclid Chemical, and the steel wire mesh used for the laminate is provided by TWP inc. The material and supplier summary is shown in Table 3. 1 below.

Table 3. 1 Materials and Suppliers

Material	Type	Supplier
Cement	Portland Type I	Clayton Concrete
Silica Fume	Densified Silica Fume	Norchem
Fine Aggregate	Concrete Sand	Clayton Concrete
Coarse Aggregate	#57 (3/4")	Clayton Concrete
Water Reducer	MasterGlenium 7620	Master Builders
Air Entrainer	MasterAir AE	Master Builders
Crack Reducer	MasterLife CRA 007	Master Builders
Micro Fibers	Polypropylene 3/4"	Euclid Chemical
Macro Fibers	Polypropylene/Polyethylene Blend 3/4"	Euclid Chemical
Steel Fibers	Crimped Steel Fibers 3/4"	Euclid Chemical

Table 3. 2 to

Table 3. 4 show the properties of the fibers used for this study, micro polypropylene, macro fibers, and steel fibers. The micro fibers are made of monofilament polypropylene, are ¾” in length, have a menlting point of 320°F, and a specific gravity of 0.91. The macro fibers are made of a blend of polypropylene and polyethylene. The specific gravity of macro fibers is 0.91, are ¾” in length, their melting point is 320°F, and have a tensile strength between 87 and 94 ksi. The material composing the steel fibers used for the study is s low carbon cold drawn steel wire, the fibers are continuously deformed circular segment, are ¾” in length and have a tensile strength ranging from 140 to 180 ksi.

Table 3. 2 Micro Fiber Properties

Material	Monofilament Polypropylene
Specific Gravity	0.91
Length	3/4"
Melting Point	320°F (160°C)

Table 3. 3 Macro Fiber Properties

Material	Polypropylene/polyethylene blend
Specific Gravity	0.91
Length	3/4"
Melting Point	320°F (160°C)
Tensile Strength	87-94 ksi
Color	Grey

Table 3. 4 Steel Fiber Properties

Material	Low carbon cold drawn steel wire
Deformation	Continuously deformed circular segment
Length	3/4"
Tensile Strength	140-180 ksi
Appearance	Bright, Clean Wire

The properties of the mesh used to fabricate the ferrocement layer are shown in Table 3. 5. The mesh have half inch squares opening, the diameter is 0.063”, their overall thickness is 0.126”, and their weight is 0.52 lb/sq foot.

Table 3. 5 Steel Mesh Properties

Mesh	2x2 per inch
Wire Diameter	0.0630"
Opening Size	0.437"
Opening Area	76%
Overall Thickness	0.126"
Weight	0.52 lb/sq foot
Weave Type	Welded
Surface Finish Coating	Mill Finish

3.3 MIX PROPORTIONS

3.3.1 Mortar

Table 3. 6 shows the mix proportions of M1H. Essentially composed of cement, sand, water and high range water reducer to achieve workability. Achieving good workability of mortar is critical in the study in order to obtain an evenly distributed material leaving no viod in the laminate. M1H is the base control mortar mix and included four ounces per cubic weight of high range water reducer. Water to cement ratio is kept constant at 0.42 for all mixes as well as cement to sand ratio at 0.5. these ratios fall in the acceptable ranges recommended for ferrocement application which are between 0.35 and 0.5 for water to cement, and 1:1.5 to 1:2.5 cement to sand (Makki, 2014).

Table 3. 6 Mix Proportions of M1H

Cement (lbs)	1095
Total Cementitious	1095
Sand (lbs)	2190
Water (lbs)	438
Super P (MG 7620) (oz/cwt)	4

Mix proportions for mix M3H are shown in Table 3. 7. Similar to M1H, but differs by the cementatious materials included. Five percent of M3H's cementitious components is silica fume and 95% is Porltand Cement. However, the use of silica fume in mortar reduces the workabilty (Antoni et. al, 2015), and for this reason in order to achieve a workable mix, the content of superplastizer is increased to six ounces per cubic weight.

Table 3. 7 Mix Proportions of M3H

Cement (lbs)	1040
Silica Fume (lbs) 5%	55
Total Cementitious	1095
Sand (lbs)	2190
Water (lbs)	438
Super P (MG 7620) (oz/cwt)	6

The mix proportions of M3HC is presented in Table 3. 8. M3HC is the same as M3H but it includes one gallon per cubic yard of crack reducing admixture used for shrinkage reduction purposes, since portland cement tends to cause high shrinkage and it is a main component in the mortar mix design.

Table 3. 8 Mix Proportions of M3HC

Cement (lbs)	1040
Silica Fume (lbs) 5%	55
Total Cementitious	1095
Sand (lbs)	2190
Water (lbs)	438
Super P (MG 7620) (oz/cwt)	6
CRA007 (gal/cu yd)	1

Table 3. 9 shows the mix proportions of M3HSC, same as M3HC but is reinforced with 0.75” crimped steel fibers a content of 0.1% by volume.

Table 3. 9 Mix Proportions of M3HSC

Cement (lbs)	1040
Silica Fume (lbs) 5%	55
Total Cementitious	1095
Sand (lbs)	2190
Water (lbs)	438
Steel Fibers (% by vol.)	0.10%
Super P (MG 7620) (oz/cwt)	6
CRA007 (gal/cu yd)	1

Table 3. 10 shows the mix proportions of M3HPC-Micro, same as M3HC but is reinforced with 0.75” micro polypropylene fibers at a content of 0.1% by volume.

Table 3. 10 Mix Proportions of M3HPC-Micro

Cement (lbs)	1040
Silica Fume (lbs) 5%	55
Total Cementitious	1095
Sand (lbs)	2190
Water (lbs)	438
Micro Fibers (% by vol.)	0.10%
Super P (MG 7620) (oz/cwt)	6
CRA007 (gal/cu yd)	1

Table 3. 11 shows the mix proportions of M3HPC-Macro, same as M3HC but is reinforced with 0.75” macro polypropylene fibers at a content of 0.1% by volume.

Table 3. 11 Mix Proportions of M3HPC-Macro

Cement (lbs)	1040
Silica Fume (lbs) 5%	55
Total Cementitious	1095
Sand (lbs)	2190
Water (lbs)	438
Macro Fibers (% by vol.)	0.10%
Super P (MG 7620) (oz/cwt)	6
CRA007 (gal/cu yd)	1

3.3.2 Class A

The mix design of the base concrete class A mix is shown in table 3.12. Class A concrete is a common mix used in the fabrication of many reinforced concrete bridge decks by transportation authorities.

Table 3. 12 Mix Proportions Concrete Class A

Cement (lb/cy)	639
Coarse Aggregate #57 (lb/cy)	1795
Sand (lb/cy)	1245
Water (lb/cy)	237
Air Entrainer (oz/cwt)	1
Super P (MG 7620) (oz/cwt)	4
Air Content (%)	8

3.4 MIXING AND SAMPLING

3.4.1 Mortar

3.4.1.1 Mortar Mixing (ASTM C305)

Mortar mixes were done according to ASTM C305. Saddle and mixing bowl used for the process are shown in Figure 3. 1 and Figure 3. 2 below. The temperature and the humidity of the room and the temperature of the mixing water were maintained at described in ASTM Specification C511. Room temperature was set at 23.0 +/- 4.0 °C, and the temperature of the mixing water used to prepare mortar mixes was 23.0 +/- 2.0 °C.

Figure 3. 1: Mortar Mixer

Figure 3. 2: Saddle for Mortar Mixer

Mixing water was first introduced in the bowl, followed by the cement, mixed for 30 seconds, and then the sand was added gradually while mixing at a slow speed. Speed increased followed by mixing for 30 seconds. Mixing paused, mortar stuck on the side of the bowl was scraped down. Finish by mixing for a minute at a medium speed (285 +/- 10 rpm)

3.4.1.2 Mortar Sampling (ASTM C109)

For every mortar mix performed over the course of this study, two inch cubes were cast for compression testing. The cubes complied with ASTM C109. Molding and tamping the test specimens was also done in accordance to ASTM C109. 3x6 cylinders samples used for splitting tensile test Free shrinkage specimens were also casted. Molds for test specimens used in determining the length change of cement pastes and mortars with the dimensions of 1 by 1 by 11.25-in in accordance with ASTM C490. Figure 3. 3 shows mortar specimens for one of the mixes performed.

Figure 3. 3 Mortar specimens

3.4.1.3 Mortar Curing and Storage (ASTM C511)

After casting, samples were cured for 24 hours while in their molds, placed in an environmental chamber and kept at a constant 74^{o}F tempreture and 50% relative humidity. After 24 hours, specimens were demolded and stored in water tanks at a temperature of 23 +/- 2 C. The water in the storage tank was saturated with lime (calcium hydroxide) to prevent leaching of calcium hydroxide as described in ASTM C511 (2013). Mortar mixes were stored in lime water tank for different number of days, 7 days. After 7 days, samples were then placed in a dry chamber where the temperature was maintained at a constant 74 ^{o}F and 50% relative humidity.

3.4.2 Concrete Class A

3.4.2.1 Concrete Mixing (ASTM C192)

Mixing and casting of samples is performed according to ASTM C192 using a 6 cubic foot capacity electric mixer. Each group of beams was of 6 beams. Prior to mixing, around 5 cubic feet of concrete are batched into 5 gallon buckets to be used for mixing. The mixer used for this part of the experiment is shown in Figure 3. 4.

Figure 3. 4 Concrete Mixer

The materials are added to the mixer separately with intervals of mixing in between. Prior to putting any of the materials into the mixer, the high-range water-reducing admixture is mixed into half the amount of the mixing water, and the air entrainer is mixed into the other half of the water. First, the coarse aggregate is put inside the mixer, followed by some of the mixing water that included the air entrainer, then add the fine aggregate, cement, and water with water reducing admixture. When the mix is ready, the beam molds are ready for casting. 6 Cylinders are cast from every group of beams in order to determine the compressive and tensile strength of the class A mix they day of beam testing, which is the 28th day after casting.

3.4.2.2 Concrete Sampling (ASTM C172)

Each mix is made in one batch with enough concrete to fill 6 beams and the required samples. Samples include two free shrinkage prisms measuring 3 x 3 x 10 inches

in addition to 6 cylinders (4x8). Sampling was done in accordance to astm C172. Specimens were filled in two layers and consolidated using vibrating tables.

3.4.2.3 Concrete Curing and Storage (ASTM C192)

In order to prevent evaporation, concrete samples are cast in plastic 4x8 cylinders with a cover, and the free shrinkage specimens in 3x3x10 inch steel prisms covered with plastic wrap. Removal of the specimens form the molds occurred after 24 hours in accordance to astm C192 (2016). To ensure a constant temperature samples are placed before and after removing from molds in a an environmental chamber kept at a constant 74 degrees Fahrenheit and 50% relative humidity. The environmental chamber is shown in Figure 3. 5.

Figure 3. 5 Environmental Chamber

3.5 LABORATORY TESTING

3.5.1 Mortar

3.5.2.2 Compressive Strength Test

Compressive strength test for mortar mixes performed on first, 7th and 28th day after casting, according to ASTM C109 (2016). 2X2 mortar cubes were tested on Forney compression machine. For every testing day, 3 cubes were tested until failure to ensure accuracy. Cubes were loaded at 35 +/- 5 psi rate.

3.5.2.3 Tensile Splitting Test

Tensile splitting test is done for the mortar mixes on first, 7th, and 28th day after casting. Specimens are placed horizontally in the testing machine as shown in Figure 3. 6 and loaded until splitting occurs. On each testing day, four samples are tested in order to achieve higher accuracy.

Figure 3. 6 Splitting Tensile Test

3.5.2.5 Free Shrinkage (ASTM C490)

Free shrinkage measurements were done in accordance to ASTM C490 (2017). For each mortar mix, two 1x1x10-in. prism concrete specimens were cast with gage studs placed at each end. The length between the two gage studs was measured in addition to the length of the reference bar using a length comparator. The specimen is slowly rotated to record the minimum reading. Three recordings for each sample at various ages were taken in order to achieve accuracy. Figure 3. 7 shows a mortar sample placed in the free shrinkage measuring machine. Length change were recorded periodically over a 56 day period.

Figure 3. 7 Mortar Free Shrinkage Specimen Measurement

3.5.2 Class A

3.5.2.2 Compressive Strength Test (ASTM C39)

Compressive strength tests performed on the 28th days after casting according to ASTM C39 (2018) standards using a sulfur based capping compound. Cylinders are sulfur-capped according to the standards set in ASTM C617 (2015) to guarantee a flat surface in order to get accurate results. The cylinder is then loaded until failure in FORNEY hydraulic compression machine with a capacity of 1,000,000 lb of force. **Figure 3. 8** shows a concrete cylinder placed in compression testing machine. Three cylinders are tested for each mix. Loading rate at 35 +/- 5 PSI, equivalent to 400 lb/s for 4X8 cylinders .

Figure 3. 8 Cylinder Placed Inside Compression Machine

3.5.2.3 Tensile Splitting Test (ASTM C496)

Tensile splitting is done for the class A mix on the day of beam flexural test, which is the 28th day after mixing, following the ASTM C496 (2017) standards. Specimens are placed horizontally in the testing machine and loaded until splitting occurs.

3.5.2.4 Modulus of Elasticity Test (ASTM C469)

ASTM C469 (2014) standards are followed for the elastic modulus test. Samples are sulfur capped. The cylinders are loaded until 40% of their compressive strength with strain readings being taken every 4,000 lb. Each cylinder is tested twice for consistency. Mix has two cylinder specimens to be tested at different age.

3.5.2.5 Free Shrinkage (ASTM C157)

According to ASTM 157 (2017), free shrinkage measurements are taken using a length comparator and prisms measuring 3 x 3 x 10 inches. Two prism samples are cast with embedded studs at either end for every mix. Samples are stored and tested in an environmentally controlled environment. The reference bar is placed into the length comparator and the length reading is taken. Then, prism sample is placed into the length comparator and the measurement is recorded. The same procedure is repeated for each sample of each mix at every testing day over the 56-day testing period.

3.6 FLEXURAL TESTING FOR STRENGTHENED BEAMS

3.6.1 Beam Preperation

Six beam molds were prepared for every group of beams cast using half inch thick plywood. Reinforcing bar is placed at a specific height, 1”, 1.25” or 1.5”. First, as seen in Figure 3. 9, the main reinforcement is placed. A strain gauge properly attached at the midspan of the rebar. Shear reinforcement is also placed and fixed as seen in Figure 3. 10. The wooden mold is then sealed around the reinforcing bar passing through. Once the reinforcements are placed and the sealer is dry, the molds are ready to be cast with the base class A mix. Figure 3. 11 shows beams with class A concrete being cast. Figure 3. 12 shows a group of beams with hardened substrate.

Figure 3. 9 Beam Molds with Main Reinforcement Rebar Placed

Figure 3. 10 Beam Molds with Shear Reinforcement Placed and Fixed

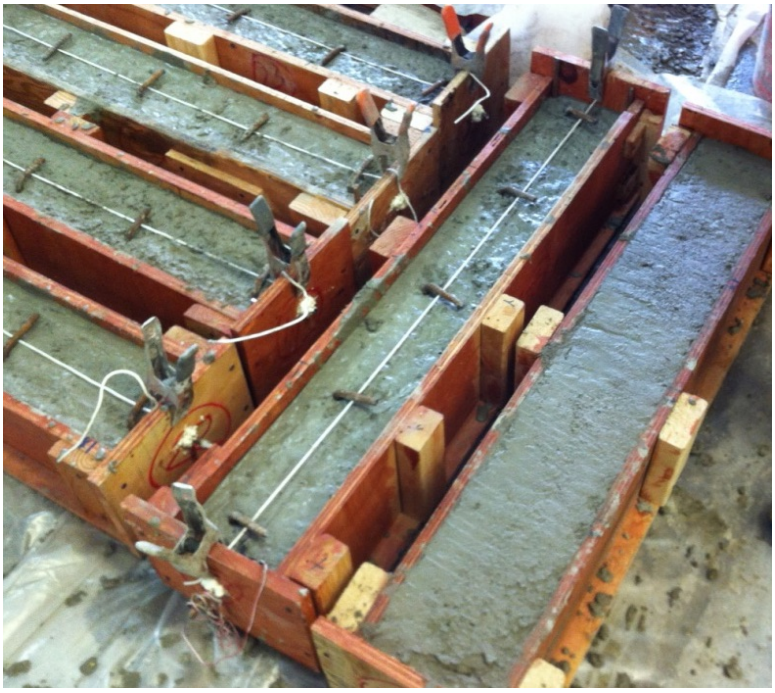

Figure 3. 11 Casting of Substrate

Figure 3. 12 Beams with Substrate

3.6.2 Casting of ferrocement repair layer

Once the class A concrete is hardened, the mesh is put in place as seen in Figure 3. 13. On the 21st day after the class A mix is cast and the after placing the mesh layers, mortar mixed and cast. After a casting, a wet burlap is placed on each beam and beams are wrapped in plastic to avoid moisture evaporation. 24 hours after the ferrocement layer is cast, the beams are demoulded and wet cured with burlap for and additional 7 days. Figure 3. 14 shows the final look of the retrofitted beams.

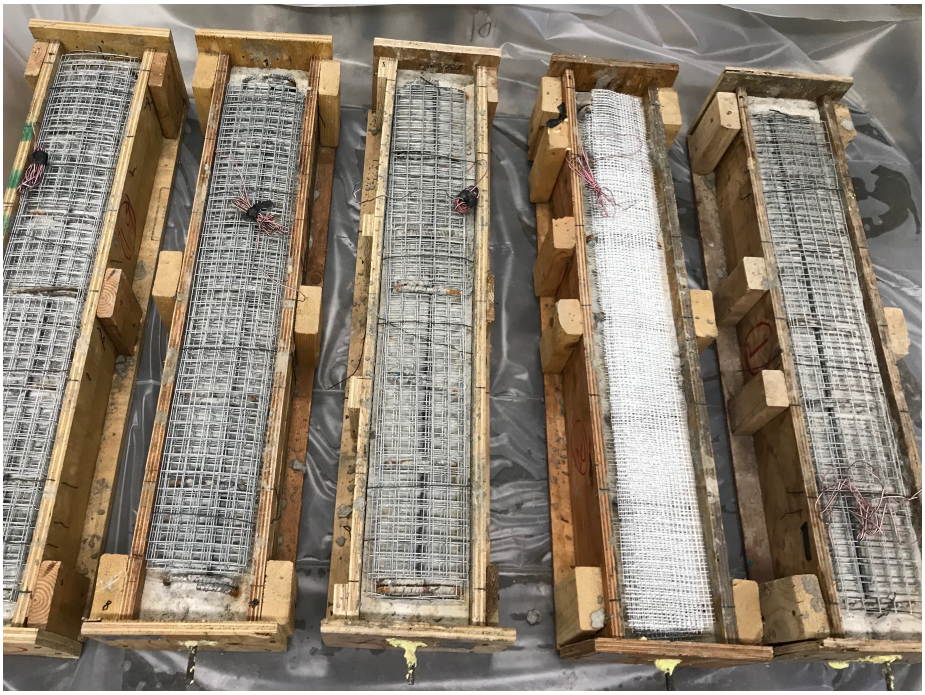

Figure 3. 13 Ferro Mesh Placed Before Casting of Mortar

Figure 3. 14 Beams with Ferrocement Laminate

3.6.3 Beam Flexural Test (ASTM C78)

Beam were simply supported and tested with third point loading system. Testing was performed in accordance to ASTM standard C78 (2018). Testing machine that was used for the study has a motorized pump with sufficient volume to complete a test in one continuous stroke without requiring refill and capable of applying loads at a uniform rate without interruption as required by the standards. Beams were tested until failure and peak load was provided by the testing machine. Strain gage was installed at the middle of the rebar before casting provided rebar strain data. Two LVDTs placed at both sides of the midspan of the beams to provide accurate deflection results during testing. Strain gage and LVDTs were connected to a data logger, which in turns was connected to a

computer that showed the readings. Figure 3. 15 shows a beam while being tested.

Figure 3. 15 Flexural Testing of Beam under Third Point Load System

3.6.3 Beams properties and details

The beam properties and details are shown in Table 3. 13. Four control beams, reinforced with a #3 rebar and 24 retrofitted beams with a ferrocement laminate are studied. Properties include the thickness of the ferrocement laminate, the number of mesh layers in the laminate, fiber content in the mortar mix used to fabricate the ferrocement layer, and the type and number of stirrups that were used to bond the two layers.

Nomenclature:

- W-X-YY-(R)-Z
- W represents the group number
- X is the number of mesh

- YY is the shear connectors and shape (#2 or #3, U or L)
- The letter R indicates the presence of a #2 rebar located at top fiber of the laminate
- Z indicates the fiber percentage by volume in the mortar mix used for the laminate

Note: 3-5-3U-Rs-0.1, (the letter “s” in the beam ID, signifies a short #2 rebar in the ferrocement layer, rebar did not span over the effective length of the beam)

3-8G-2U-R (G signifies the use of galvanized steel mesh)

Table 3. 13 Beam Properties and Details

Beam ID	*depth of concrete (in)*							Studs
		Fiber %	*b (in)*	*d (in)*	*f'cf (psi)*	*fym (psi)*	# of layers	No. & spacing
Control 1	5	-	-	-	-	-	-	-
1-0-3L-0.1	5	0.10%	6	1	6500	60	0	5#3L@9
1-1-3L-0.1(A)	5	0.10%	6	1	6500	60	1	5#3L@9
1-1-3L-0.1(B)	5	0.10%	6	1	6500	60	1	5#3L@9
1-2-3L-0.1(A)	5	0.10%	6	1	6500	60	2	5#3L@9
1-2-3L-0.1(B)	5	0.10%	6	1	6500	60	2	5#3L@9
Control 2	6	-	-	-	-	-	-	-
2-5-3L-0.1	5	0.10%	6	1	8000	60	5	7#3L@6
2-5-2U-0.1	5	0.10%	6	1	8000	60	5	7#2U@6
2-4-2U-R-0.1	5	0.10%	6	1	8000	60	4	7#2U@6
Control 3	6	-	-	-	-	-	-	7#2U@6
3-5-2U-R-0.1	5	0.10%	6	1	7000	60	5	7#2U@6
3-5-3U-Rs-0.1	5	0.10%	6	1	7000	60	5	7#3U@6
3-8-3U-R-0.1(A)	4.5	0.10%	6	1.5	7000	60	8	7#3U@6
3-8-3U-R-0.1(B)	4.5	0.10%	6	1.5	7000	60	8	7#3U@6
3-8G-2U-R-0.1	4.5	0.10%	6	1.5	7000	-	8	7#2U@6
Control 4	6	-	-	-	-	-	-	7#3U@6
4-8-3U-0.1	4.5	0.10%	6	1.5	7500	60	8	7#3U@6
4-8-3U-0.0	4.5	0	6	1.5	7500	60	8	7#3U@6
4-5-3U-0.1	5	0.10%	6	1	7000	60	5	7#3U@6
4-5-2U-0.2	5	0.20%	6	1	7500	60	5	7#2U@6
4-8-2U-0.1	4.5	0.10%	6	1.5	7000	60	8	7#2U@6
5-0-3U-0.0(A)	4.75	0	6	1.25	7500	60	0	10#3U@3
5-0-3U-0.0(B)	4.75	0	6	1.25	7500	60	0	10#3U@3
5-0-3U-0.2(A)	4.75	0.20%	6	1.25	7500	60	0	10#3U@3
5-0-3U-0.2(B)	4.75	0.20%	6	1.25	7500	60	0	10#3U@3
5-4-3U-0.2(A)	4.75	0.20%	6	1.25	7500	60	4	10#3U@3
5-4-3U-0.2(B)	4.75	0.20%	6	1.25	7500	60	4	10#3U@3

4 EXPERIMENTAL RESULTS

4.1 INTRODUCTION

The results of the compressive and tensile strength of the mortar mixes studied are evaluated in this section. The free shrinkage results from day 1 to 56 are also shown for every mortar mix. The section also shows the results of beam testing, in terms of ultimate load, deflection, cracking load and rebar strain. Cracking behavior of each beam is also presented.

4.2 FRESH CONCRETE TEST RESULTS

The slump test for the Class A concrete is performed according to the procedure described in ASTM C143 using a slump cone. For all Class A mixes, slump achieved was between 6 and 8 inches which is in the acceptable range limit.

4.3 HARDENED CONCRETE AND MORTAR TEST

4.3.1 Compressive Strength of Mortar

Table 4. 1 shows the compressive strength results of all mortar mixes at 1, 7 and 28 days of age. Results range from 4000 to 5275 PSI on the first day and from 6800 to 7230 psi on the 28^{th} day.

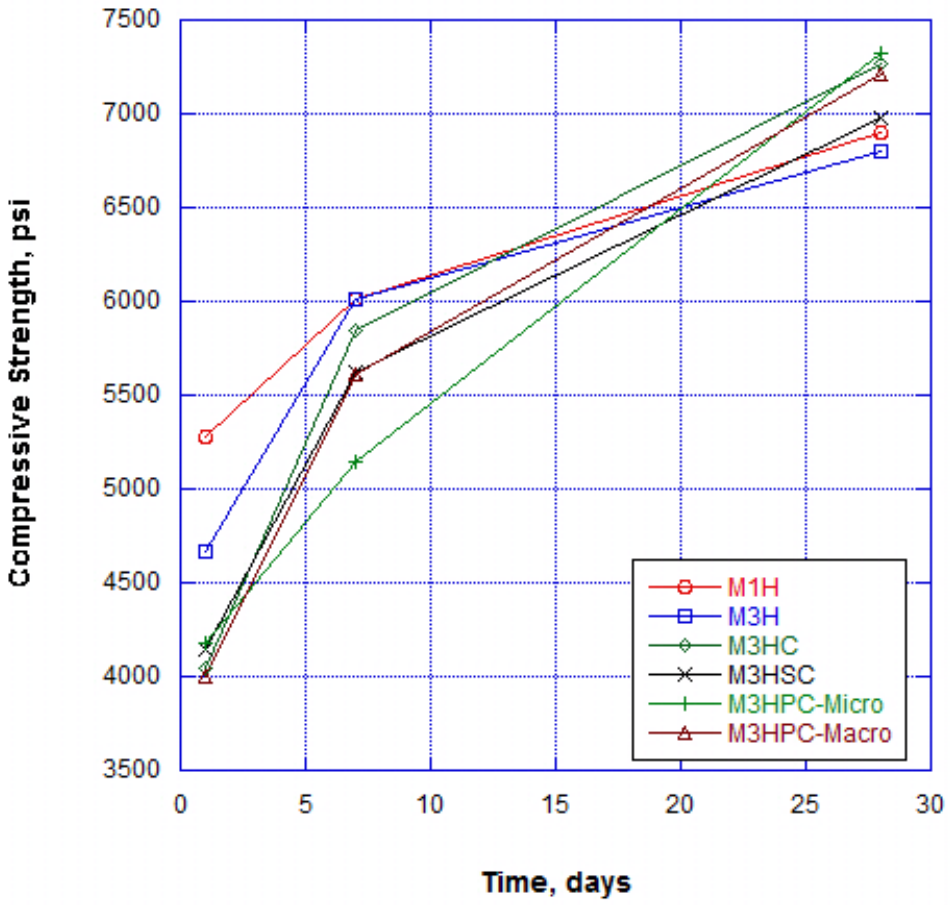

Figure 4. 1 Compressive Strength Results of Mortar Mixes

The results are also tabulated in Table 4. 1 and the comparison of strength between each two mixes are shown below in Table 4. 2 to Table 4. 6.

Table 4. 1 Compressive Strength Results of Mortar Mixes

Day	Compressive Strength (PSI)					
	M1H	M3H	M3HC	M3HSC	M3HPC-Micro	M3HPC-Macro
1	5275	4663	4050	4150	4175	4000
7	6013	6013	5850	5625	5143	5617
28	6900	6800	7269	6975	7320	7212

Table 4. 2 shows the difference in compressive strength between mortar with partial replaement of portland cement by silica fume (5%) and mortar with only portland

cement as cementitious material. The difference in strength is negligable so 5% Silica Fume as cementitious content does not affect the compressive strength of mortar.

Table 4. 2 Compressive Strength Comparison M1H, M3H

Day	Compressive Strength (PSI)		% Difference
	M1H	M3H	
1	5275	4663	-12%
7	6013	6013	0%
28	6900	6800	-1%

Table 4. 3 shows the difference in compressive strength between mortar mixes with and without Crack Reducing Admixture. For the mix that included CRA, results show a 14% decrease in strength at day 1 and 7% increase at 28 days. For this reason, we can conclude that crack reducing admixture does not affect compressive strength.

Table 4. 3 Compressive Strength Comparison M3H, M3HC

Day	Compressive Strength (PSI)		% Difference
	M3H	M3HC	
1	4663	4050	-14%
7	6013	5850	-3%
28	6800	7269	7%

The difference in compressive strength between mortar mixes with and without steel fibers is shown in Table 4. 4 and it is negligeable. The presence of steel fibers at 0.1% in the mortar mix does not affect the compressive strength.

Table 4. 4 Compressive Strength Comparison M3HC, M3HSC

Day	Compressive Strength (PSI)		% Difference
	M3HC	M3HSC	
1	4050	4150	2%
7	5850	5625	-4%
28	7269	6975	-4%

From Table 4. 5, the difference in compressive strength between mortar mixes with and without Micro Polypropylene fibers is insignificant. The presence of Micro Polypropylene fibers at 0.1% does not affect the compressive strength of mortar.

Table 4. 5 Compressive Strength Comparison M3HC, M3HPC-Micro

Day	Compressive Strength (PSI)		% Difference
	M3HC	M3HPC-Micro	
1	4050	4175	3%
7	5850	5143	-13%
28	7269	7320	1%

From Table 4. 6, the difference in compressive strength between mortar mix with and without Macro Polypropylene fiber is negligable. The addition of Macro Polypropylene fibers at 0.1% to a mortar mix does not affect the compressive strength of mortar.

Table 4. 6 Compressive Strength Comparison M3HC, M3HPC-Macro

Day	Compressive Strength (PSI)		% Difference
	M3HC	M3HPC-Macro	
1	4050	4000	-1%
7	5850	5617	-4%
28	7269	7212	-1%

4.3.2 Tensile Strength of Mortar

The tensile strength results for the mortar mixes at 1, 7 and 28 days of age are shown in Figure 4. 2 below. Results range from 339 psi to 381 psi one the first day and from 401 to 502 psi on the 28th day.

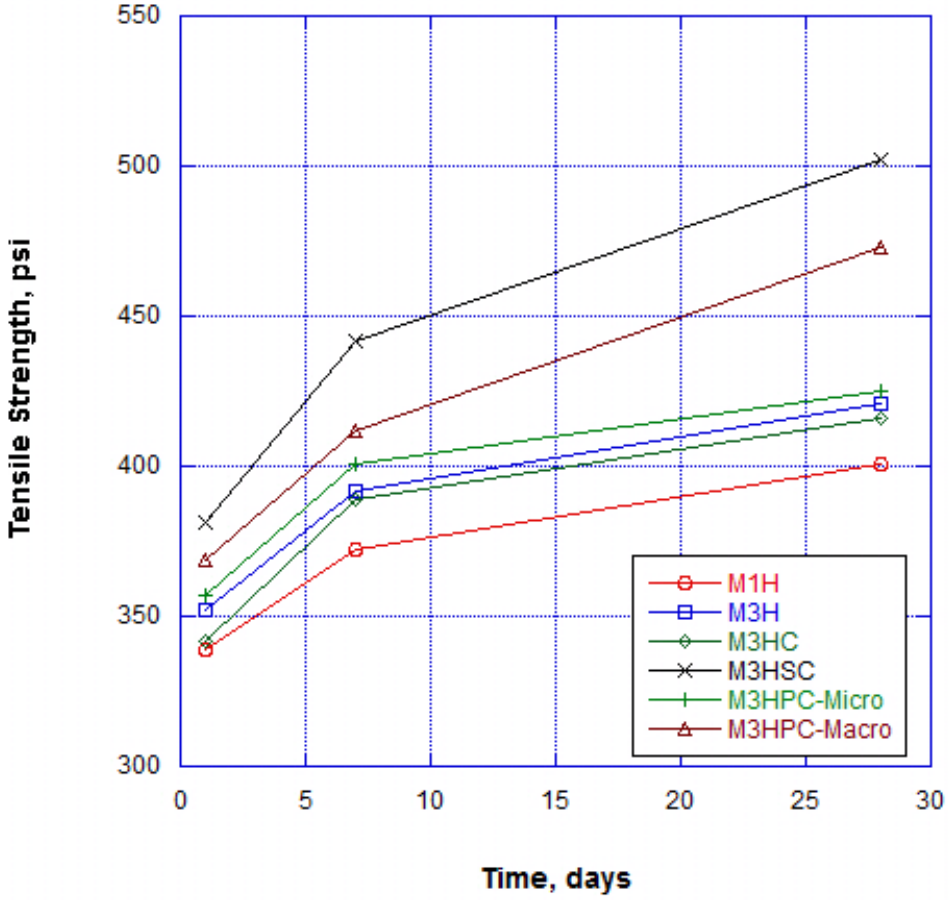

Figure 4. 2 Tensile Strength Results of Mortar Mixes

Table 4. 7 shows all the mortar mixes tensile strength results and comparison between each two mixes are detailed in Table 4. 8 to Table 4. 15.

Table 4. 7 Tensile Strength Results of Mortar Mixes

Day	Tensile Strength (PSI)					
	M1H	M3H	M3HC	M3HSC	M3HPC-Micro	M3HPC-Macro
1	339	352	342	381	357	369
7	372	392	389	442	401	412
28	401	421	416	502	425	473

Replacing 5% of the portland cement by silica fume showed 5% increase in tensile strength as shown in table 4.8. On the 28th day, M1H (control mix)'s tensile strength was 401 psi and M3H, which includes 5% silica fume of it's cementitious material failed at 421 psi.

Table 4. 8 Tensile Strength Comparison M1H, M3H

Day	Tensile Strength (PSI)		% Difference
	M1H	M3H	
1	339	352	4%
7	372	392	5%
28	401	421	5%

Including crack reducing admixture in the mortar mix design does not affect the tensile strength. Table 4. 9 shows that the difference in tensile strength for mortar mixes with and without crack reducing admixutre is negligeable.

Table 4. 9 Tensile Strength Comparison M3H, M3HC

Day	Tensile Strength (PSI)		% Difference
	M3H	M3HC	
1	352	342	-3%
7	392	389	-1%
28	421	416	-1%

Table 4. 10 below shows the difference in terms of tensile strength of mortar mixes with and without crimped steel fiber. The addition of 0.1% of crimped steel fibers (0.75" in length) increased the tensile strength of the mortar by 10% on the first day, 11% on the 7th day and 17% on the 28th day.

Table 4. 10 Tensile Strength Comparison M3HC, M3HSC

Day	Tensile Strength (PSI)		% Difference
	M3HC	M3HSC	
1	342	378	10%
7	389	435	11%
28	416	494	17%

Table 4. 11 below shows the difference in terms of tensile strength of mortar mixes with and without micro polypropylene fibers. The addition of 0.1% of micro polypropylene fibers (0.75" in length) increased the tensile strength of the mortar by 4% on the first day, 3% on the 7th day and 2% on the 28th day. 0.1% of micro fibers does not cause a significant increase in tensile strength because they are meant to enhance shrinkage perforcmance but do not have an impact on tensile strength.

Table 4. 11 Tensile Strength Comparison M3HC, M3HPC-Micro

Day	Tensile Strength (PSI)		% Difference
	M3HC	M3HPC-Micro	
1	342	357	4%
7	389	401	3%
28	416	425	2%

Table 4. 12 below shows the difference in terms of tensile strength of mortar mixes with and without macro polypropylene fibers. The addition of 0.1% of micro polypropylene fibers (0.75" in length) increased the tensile strength of the mortar by 8%

on the first day, 6% on the 7th day and 13% on the 28th day. The addition of 0.1% of macro polypropylene fibers has a positive impact on the tensile strength of mortar.

Table 4. 12 Tensile Strength Comparison M3HC, M3HPC-Macro

Day	Tensile Strength (PSI)		% Difference
	M3HC	M3HPC-Macro	
1	342	369	8%
7	389	412	6%
28	416	473	13%

Table 4. 13 below shows the difference in terms of tensile strength of mortar mix with micro polypropylene and mortar mix with crimped steel fibers. Mortar mix with steel fiber experenced higher results in tension by 7% on the first day, 10% on the 7th day and 17% on the 28th day.

Table 4. 13 Tensile Strength Comparison M3HSC, M3HPC-Micro

Day	Tensile Strength (PSI)		% Difference
	M3HSC	M3HPC-Micro	
1	381	357	-7%
7	442	401	-10%
28	502	425	-17%

Table 4. 14 below shows the difference in terms of tensile strength of mortar mix with micro polypropylene and mortar mix macro polypropylene fibers. Mortar mix with macro polypropylene experenced higher results in tension by 3% on the first day, 3% on the 7th day and 11% on the 28th day.

Table 4. 14 Tensile Strength Comparison M3HPC-Macro, M3HPC-Macro

Day	Tensile Strength (PSI)		% Difference
	M3HPC-Micro	M3HPC-Macro	
1	357	369	3%
7	401	412	3%
28	425	473	11%

Table 4. 15 below shows the difference in terms of tensile strength of mortar mix with macro polypropylene and mortar mix with crimped steel fibers. Mortar mix with steel fiber experenced higher results in tension by 3% on the first day, 7% on the 7th day and 6% on the 28th day. Steel fibers are more effective than macro polypropylene in terms of their effect on the tensile strength of the mortar.

Table 4. 15 Tensile Strength Comparison M3HSC, M3HPC-Macro

Day	Tensile Strength (PSI)		% Difference
	M3HSC	M3HPC-Macro	
1	381	369	-3%
7	442	412	-7%
28	502	473	-6%

4.3.3 Mortar Mixes Free Shrinkage Results

The free shrinkage results for the mortar mixes are shown in Figure 4. 3. For the six mortar mixes studied, the change in length is recorded over a period of 56 days. Free shrinkage results on the 56th day ranged from 590 to 788 microstrain. Table 4.16 shows the change in length for every mortar mix on the 56th day and the difference with the control mix. In this section, the effects of 5% silica fume replacement and the addition of crack reducing admixture on the change in length will be shown. In addition, the effect of

the three types of fibers that were used in this study on the free shrinkage results will also be shown.

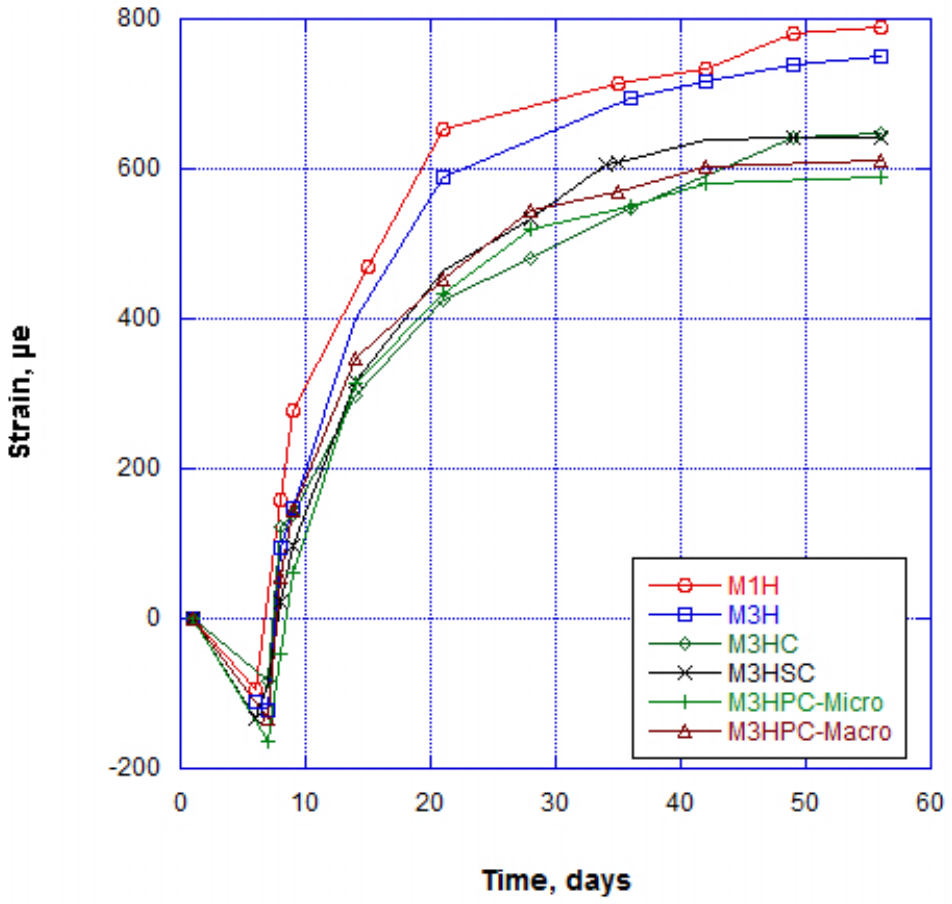

Figure 4. 3 Mortar Mixes Free Shrinkage Results

From Table 4. 16 we can see that the mortar mix that shrank the most is M1H, which is the control mix made of cement, sand, water, and high range water reducer, with 788 microstrain at 56 days. Followed by M3H which only differs from M1H by 5% of its cementitious materials that is silica fume. M3H reached 749 microstrain at 56th days, 5% less than the control mix. However, when crack reducing admixture was added to the mix design, there was an 18% decrease in shrinkage at 56 days, shown by mix M3HC with 647 microstrain. M3HPC-micro, which included micro polypropylene fibers, shrank the

least with 590 microstrain at 56 days. M3HSC, which included steel fibers experienced a higher change in length when compared to the mortar mixes reinforced by macro or micro polypropylene, with 641 microstrain at 56 days.

Table 4. 16 Free Shrinkage Results and Comparison with M1H

MIX ID	Shrinkage at 56 days (με)	% Difference with M1H
M1H	788	NA
M3H	749	-5%
M3HC	647	-18%
M3HSC	641	-19%
M3HPC-Micro	590	-25%
M3HPC-Macro	610	-23%

4.3.4 Mechanical Properties of hardened concrete

Class A concrete compressive strength, tensile strength and modulus of elasticity results are tabulate in Table 4. 17 shown below. On the day of beam testing, the Class A compressive strength was 4172 psi and tensile strength 442 psi.

Table 4. 17 Compressive Strength, Tensile Strength and Modulus of Elasticity of Concrete

Day	Compressive Strength (PSI)	Tensile Strength (PSI)	Modulus of Elasticity (PSI)
1	2480	281	3375
3	2671	334	3821
7	3288	353	3645
14	3559	366	3818
28	4172	442	4134
56	4578	429	4020

4.3.5 Free Shrinkage Results of Class A Concrete

The class A concrete free shrinkage results are shown in Figure 4. 4 for three different curing method; dry curing, 7 day wet curing in tank, and 7 day wet curing in burlap. On the 56th day the dry cured samples had the highest change in length with 490 microstrain while wet cured samples in tank had 450 microstrain and the wet cured samples under burlap had a change in length of 460 microstrain. For the purpose of this study, all beams were cured under wet burlap for seven days to achieve reasonable shrinkage results while still taking an approach that could be implemented in real life application.

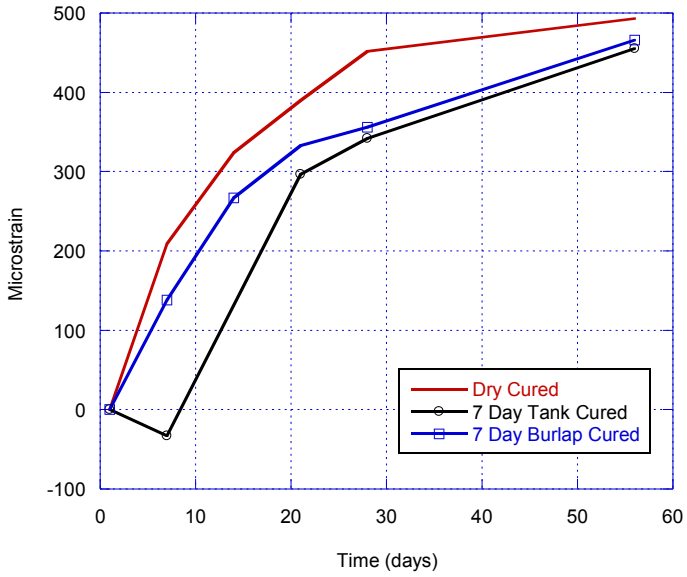

Figure 4. 4 Free shrinkage results for concrete Class A

4.4 FLEXURAL TEST RESULTS FOR BEAMS

4.4.1 Cracking and ultimate load

Table 4. 18 shows a summary of the beam testing results. For each beam, the cracking load, the deflection at the cracking load, the ultime load, the deflection at the ultimate load, and the number of cracks in recorded. In addition, the stirrups type, size, and spacing is shown. Each group has a variable that was investigated. The first group evaluated the effect of zero, one, and two mesh in the ferrocement layer. The second group compared the effect of having five mesh layers to four with a #2 rebar, as well as the difference between using #3 L shaped stirrups and #2 U shaped stirrups. The third group of beams compared the difference between the effect of 1.5" laminates with eight mesh layers, to 1" thick laminates with five mesh layers. The fourth group of beams studied the effect of fiber content at different percentages. The fifth and last group of beams showed the effect of fibers only in the ferrocement in comparison to fibers and mesh layers in the laminate.

Table 4. 18 Beams testing results summary

Beam ID	Studs Spacing (in)	Cracking Load (Kilopounds)	Deflection (in)	Ultimate Load (Kilopounds)	Deflection (in)	# of cracks
Control 1	-	4.9	0.023	7.8	0.445	2
1-0-3L-0.1	9	4.4	0.057	8.2	0.45	5
1-1-3L-0.1(A)	9	4.2	0.058	7.3	0.642	4
1-1-3L-0.1(B)	9	4.7	0.033	7.2	0.368	4
1-2-3L-0.1(A)	9	5.6	0.038	9.2	0.181	6
1-2-3L-0.1(B)	9	4.2	0.053	7.5	0.518	4
Control 2	-	3.6	0.026	7.4	0.537	3
2-5-3L-0.1	6	5.8	0.047	9.6	0.238	5
2-5-2U-0.1	6	4.4	0.027	7.5	0.451	4
2-4-2U-R-0.1	6	5.6	0.051	10.2	0.229	3
Control 3	6	3.2	0.032	7.1	0.719	3
3-5-2U-R-0.1	6	6.9	0.062	13.2	0.303	3
3-5-3U-Rs-0.1	6	6.2	0.089	10.8	0.404	3
3-8-3U-R-0.1(A)	6	7.4	0.12	13.2	0.554	4
3-8-3U-R-0.1(B)	6	8.4	0.051	14	0.622	5
3-8G-2U-R-0.1	6	6.5	0.072	13.8	0.196	7
Control 4	6	3.8	0.032	8.5	0.427	3
4-8-3U-0.1	6	7.7	0.035	12.7	0.217	4
4-8-3U-0.0	6	5.1	0.043	9.6	0.181	4
4-5-3U-0.1	6	10.2	0.055	15.4	0.196	4
4-5-2U-0.2	6	8.4	0.063	13.1	0.182	3
4-8-2U-0.1	6	8	0.025	17.7	0.24	8
5-0-3U-0.0(A)	3	3.8	0.024	6.7	0.479	3
5-0-3U-0.0(B)	3	4.2	0.03	7.6	0.561	3
5-0-3U-0.2(A)	3	4.1	0.05	8.1	0.549	3
5-0-3U-0.2(B)	3	4.4	0.059	7.4	0.621	3
5-4-3U-0.2(A)	3	8.7	0.053	13.2	0.197	7
5-4-3U-0.2(B)	3	9.5	0.051	13.4	0.182	5

4.4.2 Load vs Deflection

Group 1: All beams from group 1 failed in flexure. Figure 4. 5 shows the applied load versus the midspan deflection for that group of beams. 1-2-3L-0.1(A) achieved the highest ultimate load at 9.2 kips, and experienced the first crack at 5.6 kips. 1-2-3L-0.1(A) had two mesh layers in the ferrocement laminate. All beams from this set had the same type and spacing of stirrups, five #3 L-shaped equally spaced along the effective length. The other beams from group 1, control, beams with 0 mesh in laminate (1-0-3L-0.1), and beams with 1 mesh in laminate (1-1-3L-0.1), had their first crack at a similar load, ranging from 4.2 to 4.9 kips, and their ultimate load ranged from 7.2 to 7.8 kips. A laminate with no mesh or with one mesh only does not show an improvement in the performance of the retrofitted beam, not in terms of cracking load nor ultimate load when compared to control beam. However, all beams of this group showed ductile behavior similar to the control beam.

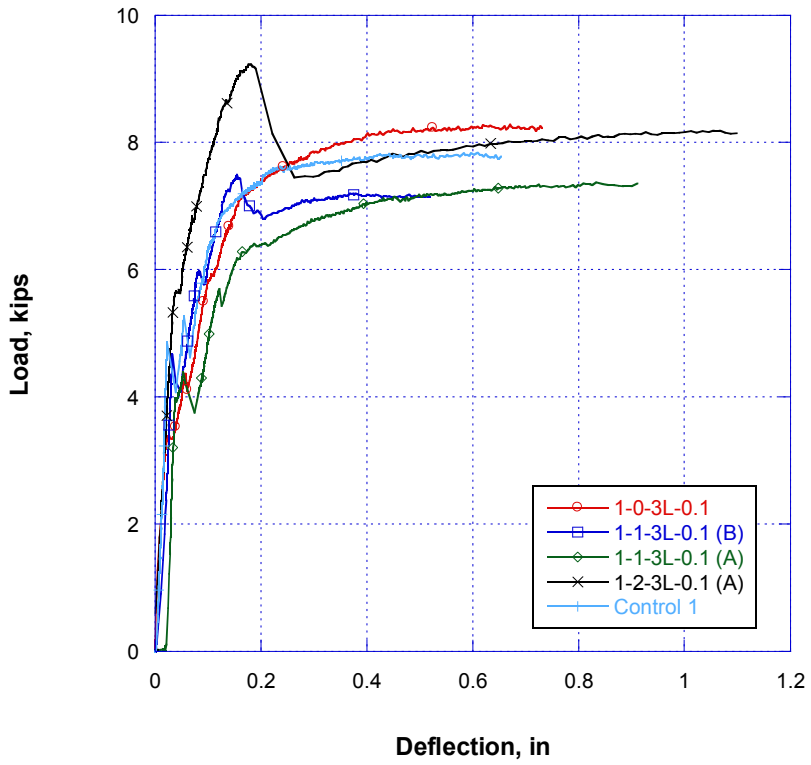

Figure 4. 5 Load VS Mispan Deflection Group 1

Group 2: The applied Load versus midspan deflection results are shown in Figure 4. 6. For the second group of beams, 2-4-2U-R, experienced the highest ultimate load of 10.2 kips, 30% increase compared to control beam which failed at 7.4 kips. 2-4-2U-R had a #2 rebar embedded in the laminate. 2-5-3L had an ultimate load of 9.6 kips, 20% higher than control beam's ultimate load. All beams had higher cracking and ultimate load compared to the control beam of that group. 2-5-2U did not experience a considerably higher load with comparison to the control beam, only 8% higher. 2-5-3L and 2-4-2U-R had almost the same cracking load, ultimate load and deflections at both stages. Ferrocement layer on the tension side of the reinforced concrete beam delayed cracking and aided in reaching a higher ultimate load than that of the control beam.

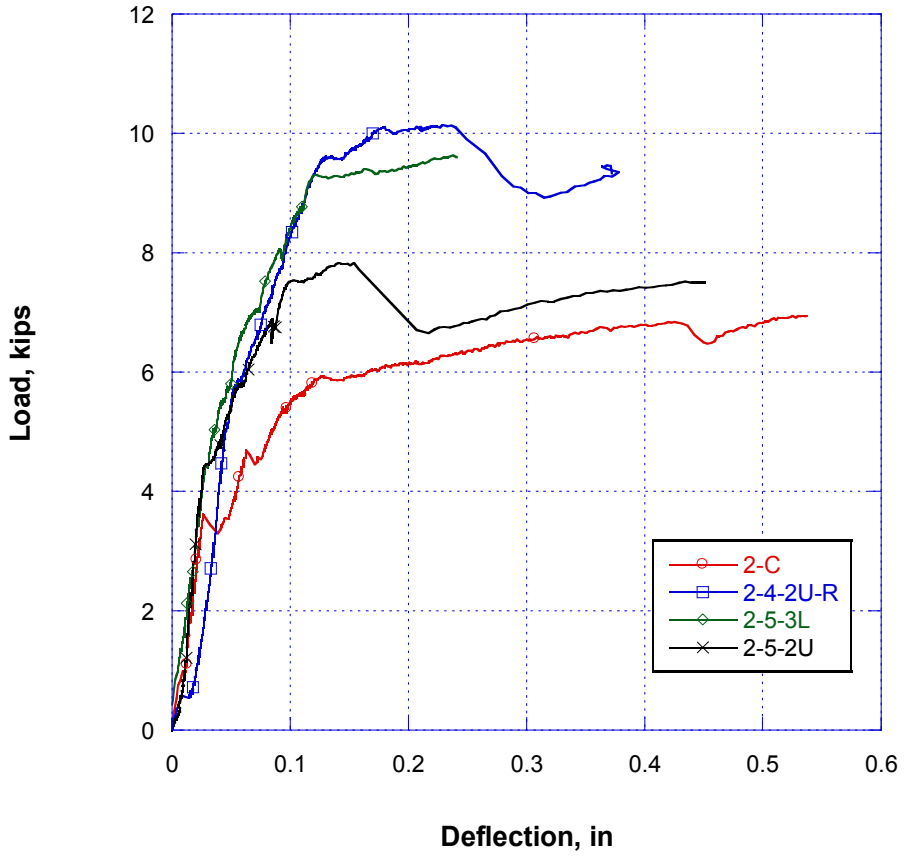

Figure 4. 6 Load VS Midspan Deflection Group 2

Group 3: Load versus midspan deflection results for group 3 are shown in Figure 4. 7. Beams from this group had a #2 rebar imbedded in the ferrocement layer. Some beams had #3 U shaped stirrups while others had #2 U shaped stirrups. Beams from this group had either 5 or 8 meshes in the repair layer. All of these beams performed better in terms of cracking load and ultimate load compared to the control beam. The increase in cracking load for these beams compared to the control beam ranged from 94% to 162%, while the increase in ultimate load ranged from 52% to 95%. 3-8-3U-R-0.1 (A) had the highest ultimate load. Beam (3-8G-2U-R), had galvanized steel mesh, reached an ultimate load of 13 kips, but it experienced a flexural shear failure, which occurred

suddenly with a separation of the two layers. 3-5-3U-Rs-0.1 failed in flexure, experienced a brittle failure because the #2 rebar located in the repair layer wasn't placed well, it didn't reach the full effective length of the beam and was sticking out on one end. This explains the poor performance of beam 3-5-3U-Rs-0.1. Furthermore, 3-8-3U-R-0.1 (A) and (B), which were identical beams, experienced the same pattern of cracking load, ultimate load and ductility. All beams with exception to those that failed in shear experienced a sudden drop in load after reaching ultimate and had a behavior similar to the control beam.

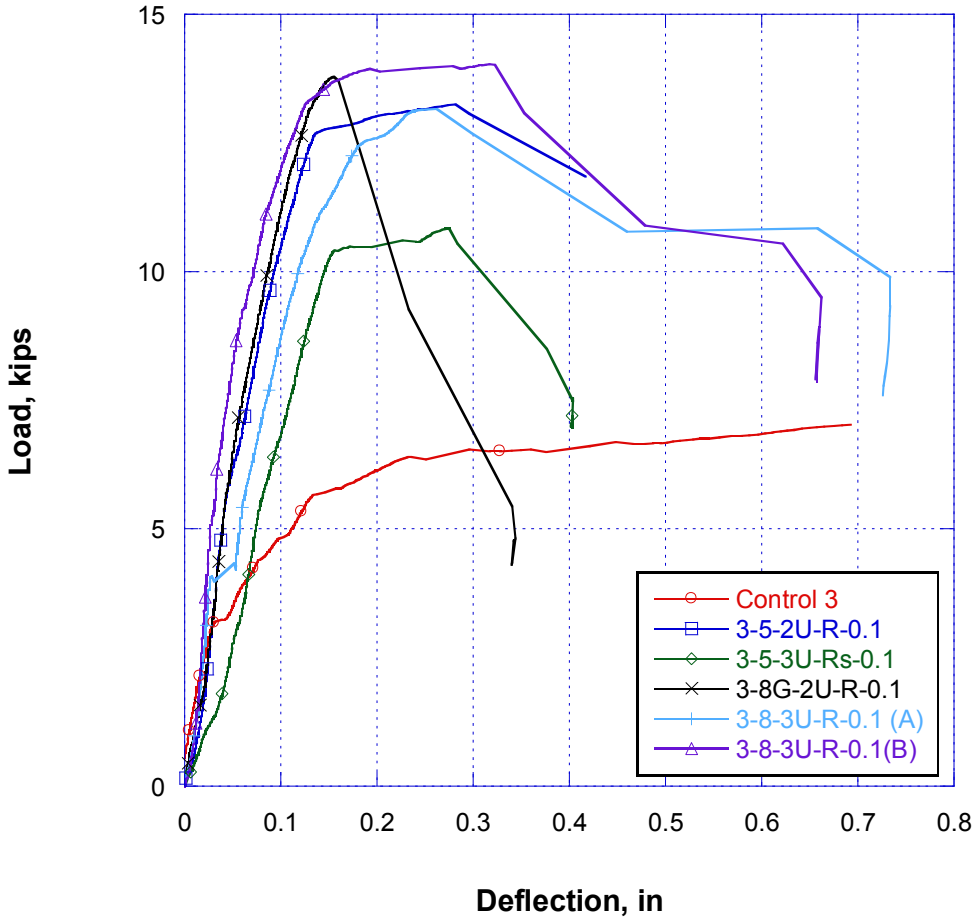

Figure 4. 7 Load VS Midspan Deflection Group 3

Group 4: Applied load versus midspan deflection for beams of group 4 shown in Figure 4. 8. Control beam from group 4 cracked at 3.8 kips and reached an ultimate load of 8.5 kips. Beams from this group differed by their fiber content, size of stirrups, and thickness of ferrocement laminate, number of mesh. All beams showed better performance in terms of cracking and ultimate load, ranging from a 34% to 168% increase in cracking load (compared to control beam) and 14% to 109% in terms of ultimate load. The beam with the least increase in strength was 4-8-3U-0.0, which did not include any macro polypropylene fibers in the ferrocement layer. 4-8-3U-0.0 had a 34% higher cracking load and 14% higher ultimate load than that of the control beam. 4-8-3U-0.0 failed in shear with a seperation of the laminate and substrate occuring after reaching the ultimate load. Deflection of beams from group 4 was reduced by 43.8% to 57.6% comparing to deflection of control beam.

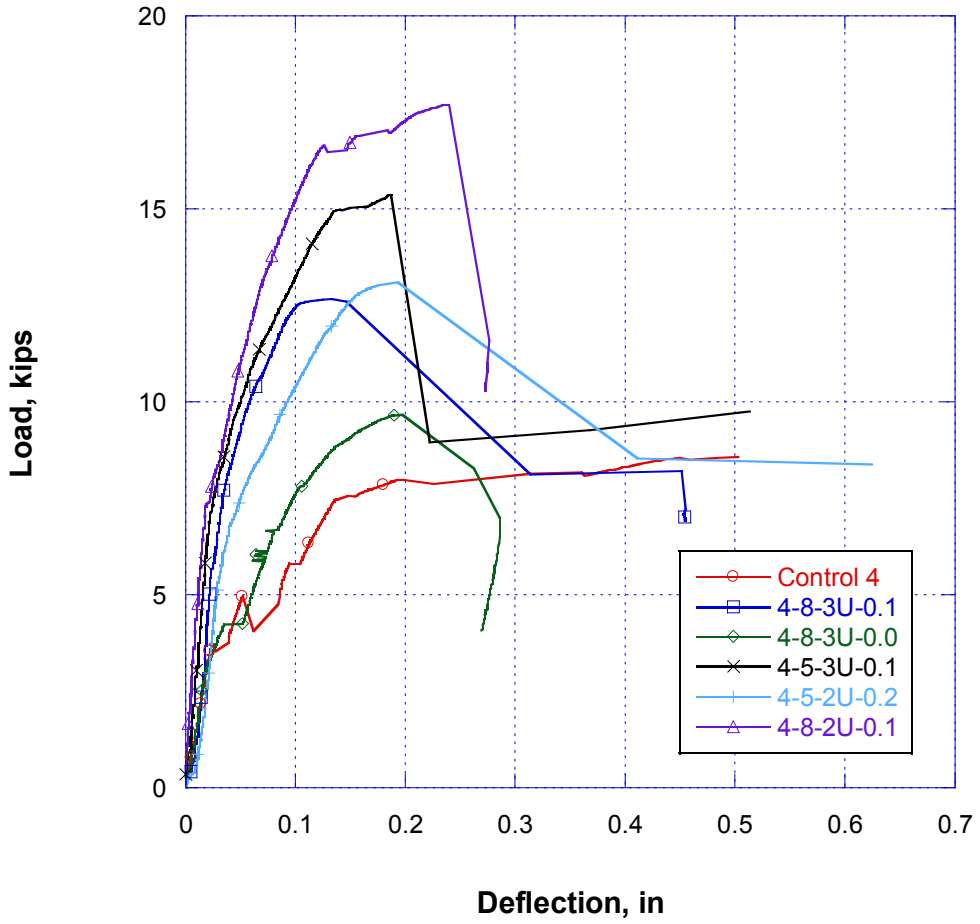

Figure 4. 8 Load VS Midspan Deflection Group 4

Group 5: Load versus midspan deflection results are shown in Figure 4. 9. All beams in group 5 shared the same shear reinforcement and thickness of laminate. This group included two beams with no fiber or mesh in their laminate, two beams with no mesh and 0.2% macro polypropylene fibers 0.75" in length, and two beams with 4 mesh layers and 0.2% macro polypropylene fibers 0.75" in length. The graph above shows the applied load versus displacement for these beams. Beams with mesh in their laminate naturally performed better in strength and cracking with 114% increase in cracking load and 71% increase in ultimate load when compared to beams with no mesh or fibers in

their laminate. Normally, we could say that the presence of steel mesh in the laminate affects greatly the performance of the beam. Furthermore, when comparing beams that didn't include any mesh, those with fibers to those without fibers, we see a negligible increase in cracking load, 6%, and an increase of 9% in ultimate load.

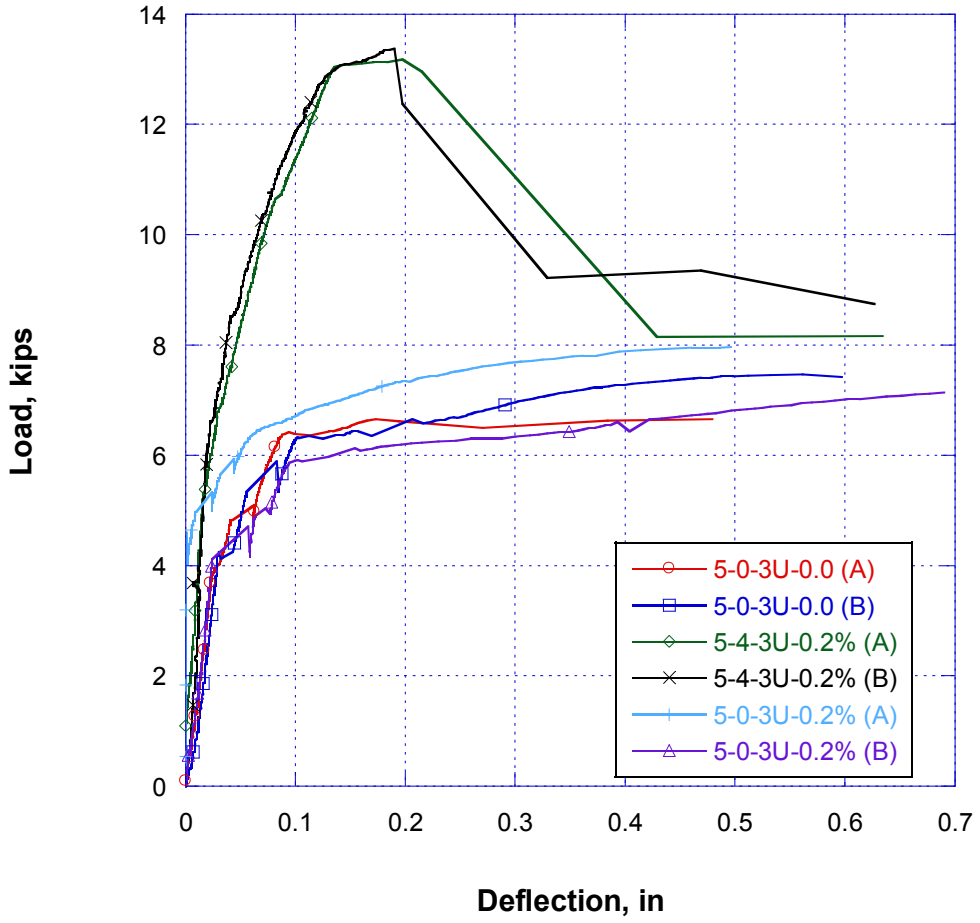

Figure 4. 9 Load VS Midspan Deflection Group 5

4.4.3 Load vs Rebar Strain

Figure 4. 10 shows the applied load versus the strain in the middle of the main reinforcing bar. As illustrated in the graph, the main steel reinforcement in every beam specimen has reached the yield strength of 0.002 at ultimate load except for beam 3-5-3U-Rs-0.1 which failed in shear. 3-5-3U-Rs-0.1 performed poorly due to the

misplacement of the #2 rebar in the laminate, experiencing sudden britlle failure with a seperation of the layers. Also, as seen in the graph (Figure 4. 10), all retrofitted beam' rebars yielded at a higher load compared to control beam. We can conclude that the ferrocement layer delayed the yeilding of the reinforcing bar significantly by handling tension load.

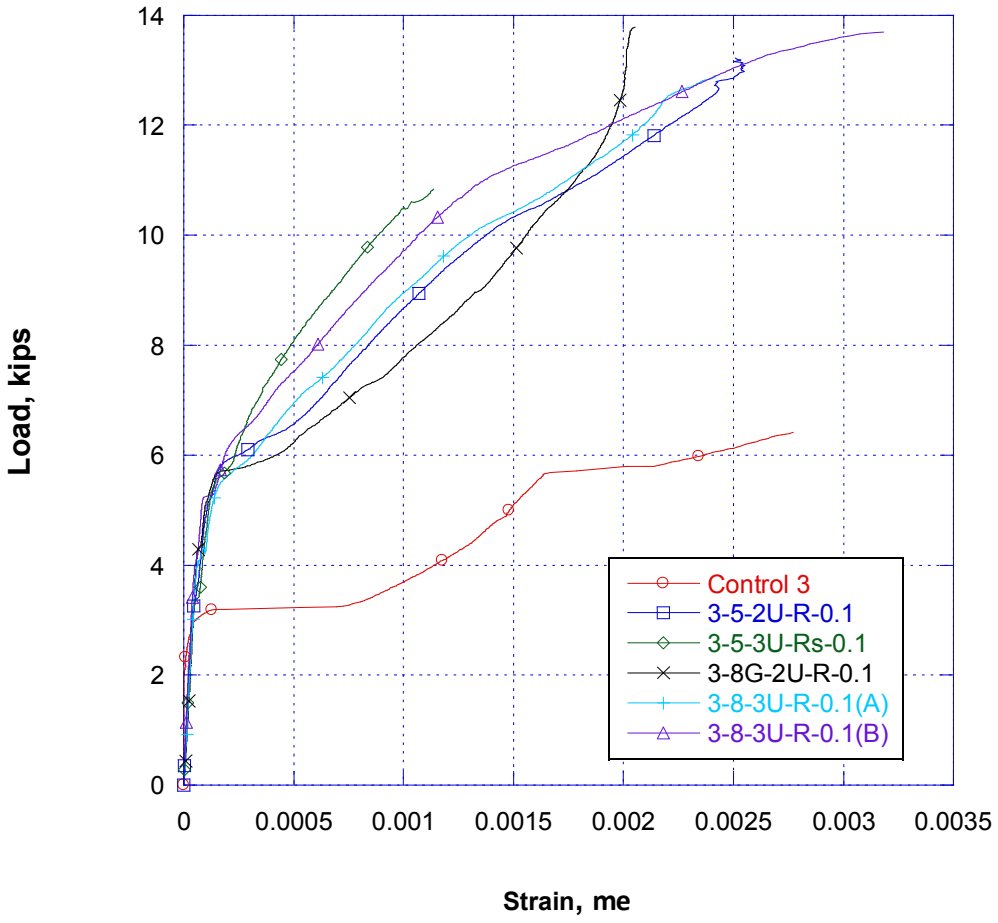

Figure 4. 10 Load VS Rebar Strain Group 3

Group 4: For the 4th group of beams, Figure 4. 11 shows the applied load versus the strain in the middle of the main reinforcing bar. As shown in the graph, the main steel reinforcement in every beam specimen has reached the yield strength of 0.002 at ultimate

load. All retrofitted beam' rebars yielded at a considerably higher load compared to control beam. We can conclude that the ferrocement layer delayed the yeilding of the reinforcing bar by its effectiveness in carrying tensile load.

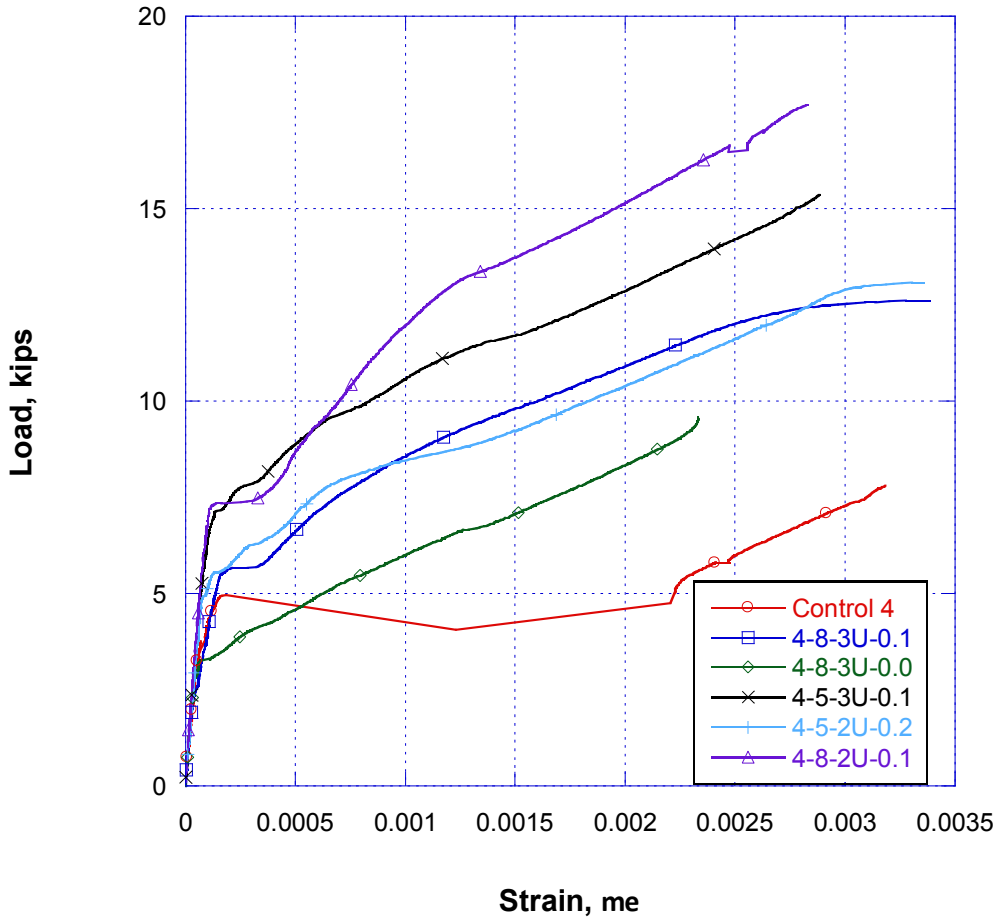

Figure 4. 11 Load VS Rebar Strain Group 4

Group 5: Figure 4. 12 shows the applied load versus the strain for group 5 of beams. As illustrated in the graph, the main steel reinforcement in every beam specimen has reached the yield strength of 0.002 at ultimate load except for beam 5-0-0.0(A) which failed in shear. 5-0-0.0(A) did not include any fibers or mesh in the laminate and failed with a seperation of the layers. Retrofitted beams with mesh in the laminate, or fibers alone, had

their rebar yielded at a considerably higher load compared to beams with no mesh or fibers in their laminate. We can conclude that the ferrocement layer delayed the yeilding of the reinforcing bar by its effectiveness in carrying tensile load. However, a laminate with no mesh or fibers does not delay the yielding of the steel and is therefore not effective in retrofitting beams.

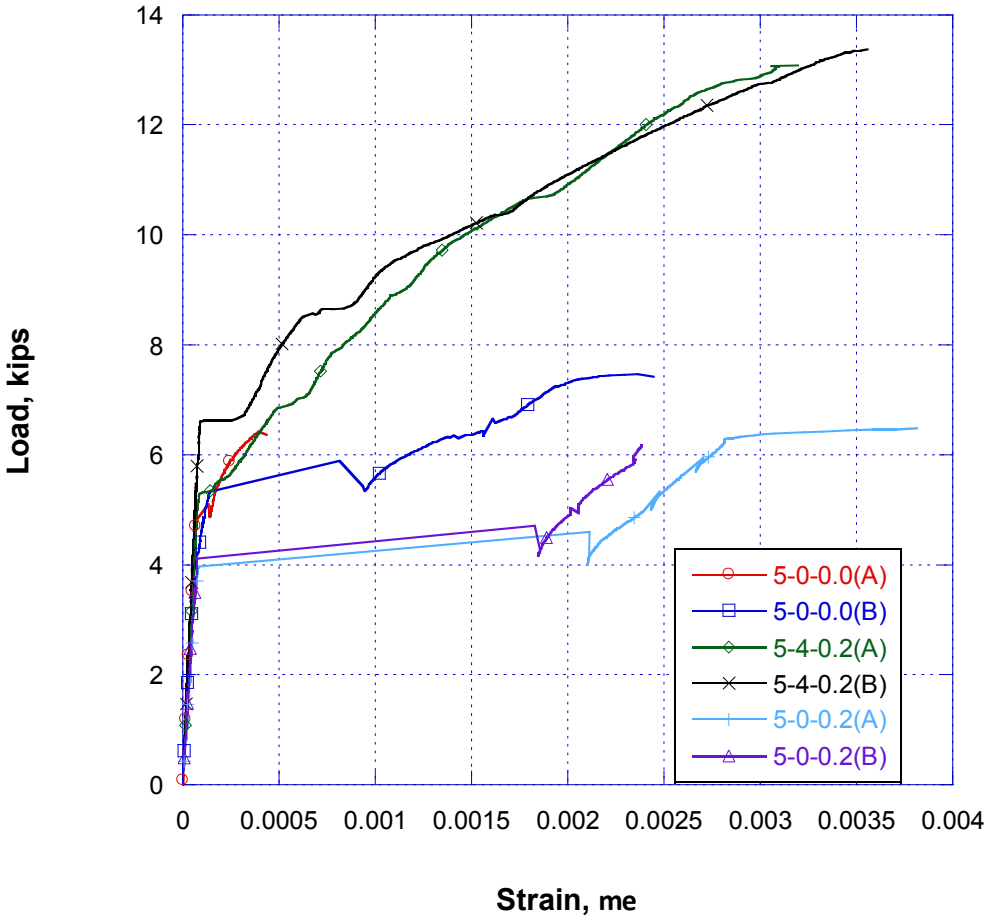

Figure 4. 12 Load VS Rebar Strain Group 5

4.4.4 Cracking Behavior

Group 3: Cracking load for retrofitted beams increased by 94%-163%. Beams with #3 studs cracking load increased by 133-163% while beams with #2 studs cracking load increase by 94-103%. Beam with galvanized mesh had 7 cracks while other beams had 3-5 cracks, signifying a better stress distribution. Beams with #2 studs had less cracks than the beams with #3 studs. Figure 4. 13 shows the crack maps of beams from group 3.

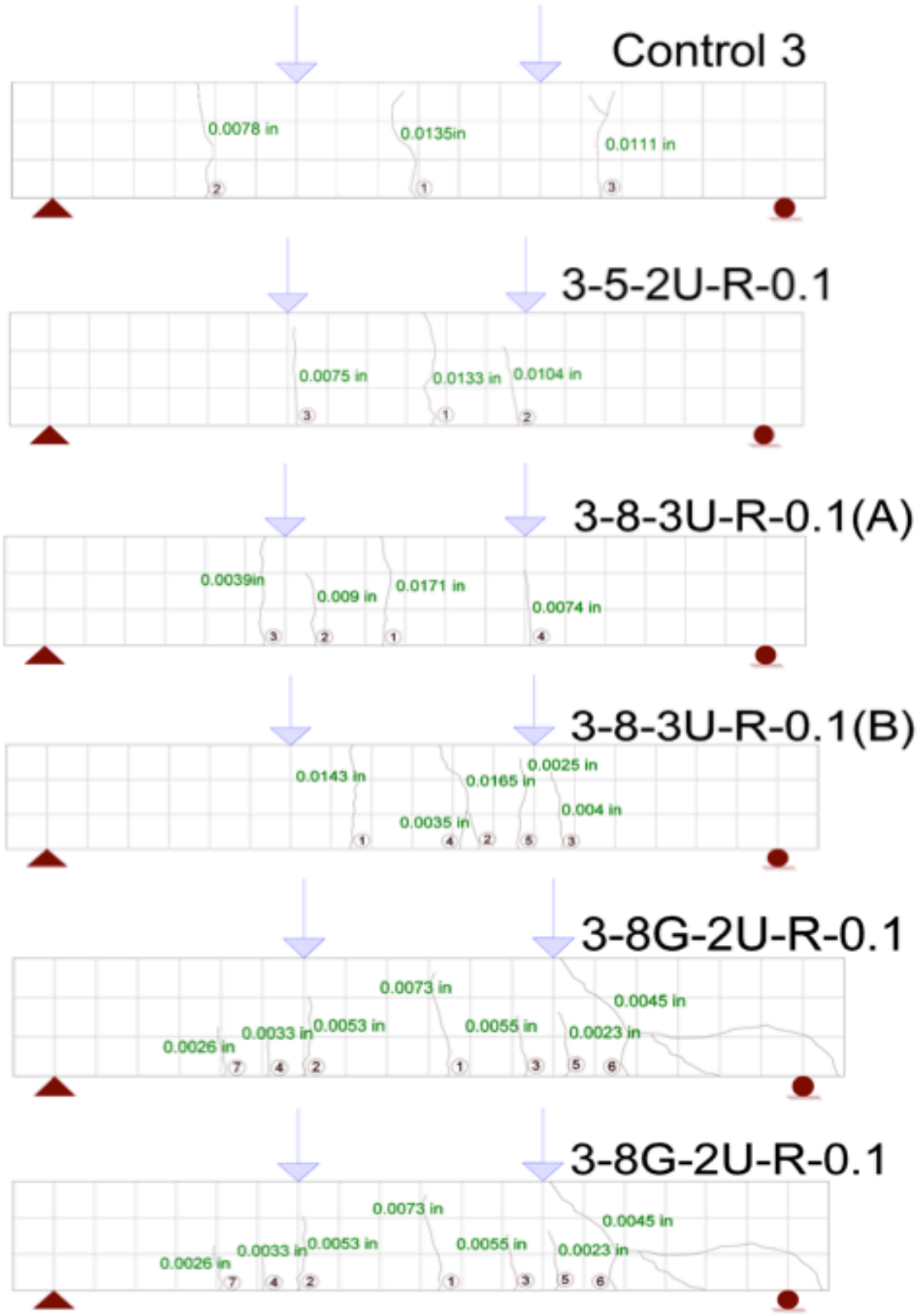

Figure 4. 13 Crack Maps of Group 3 beams

Group 4: 4-5-2U-0.2 with 0.2% fibers and #2 studs had less cracks compared to beam 4-5-3U-0.1 with 0.1% fibers and #3 studs, however thickness of cracks at failure were similar. 4-8-3U-0.1 with 0.1% fiber had thinner cracks at failure (25%) when compared to same beam but without fibers (4-8-3U-0.0) Cracking load for beams with #3 studs was 14% greater than beams with #2 studs. Figure 4. 14 shows the cracks of beams of Group 4.

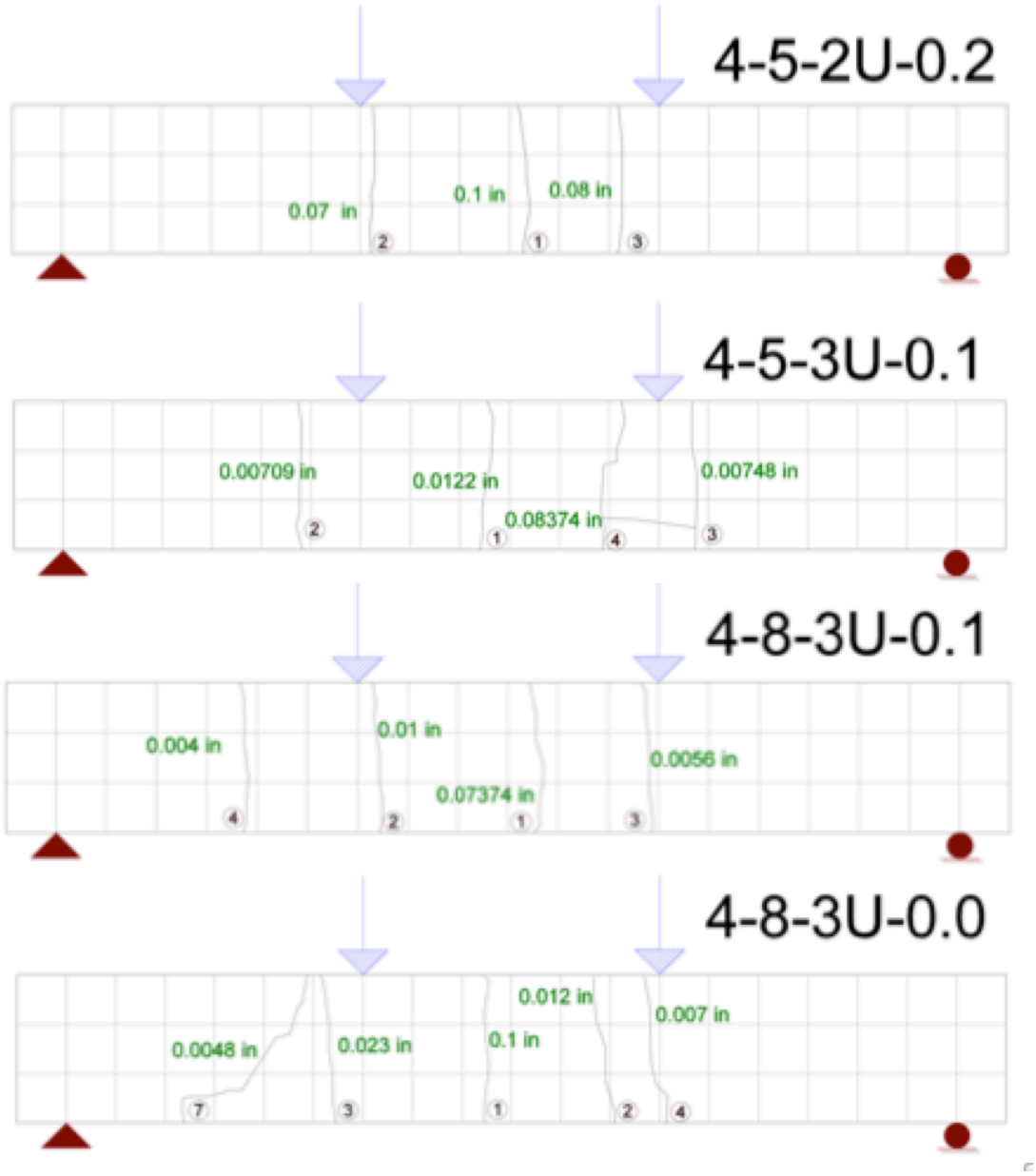

Figure 4. 14 Crack Maps of Group 4 Beams

Group 5: Beams with no fibers and no mesh in the laminate had large crack width at failure. For specimens without mesh, the addition of 0.2% macro polypropylene fibers did not have a significant impact on the crack width at failure. The use of 4 mesh in

addition to 0.2% fibers led to a decrease in crack width at failure, an increase in the number of cracks, better stress distribution. Figure 4. 15 displays the crack maps of beams from group 5.

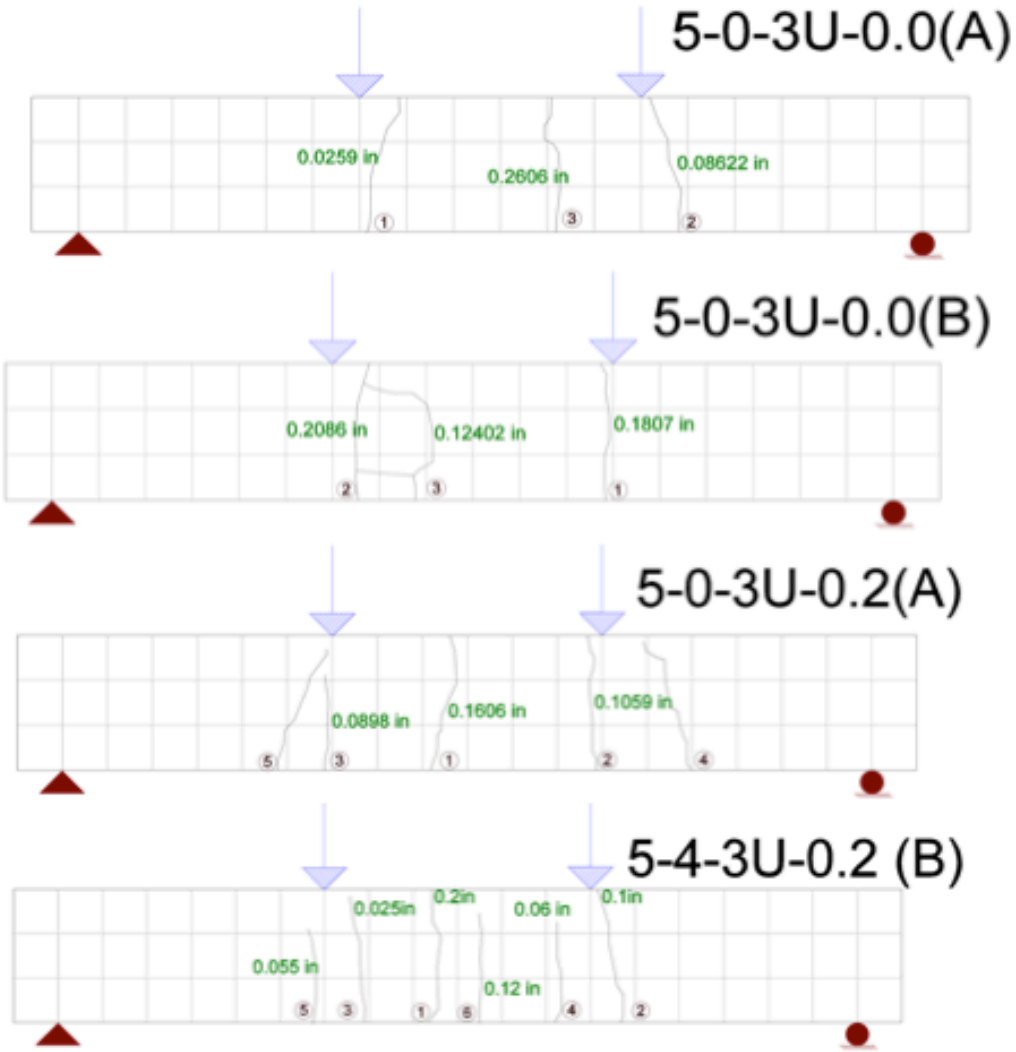

Figure 4. 15 Crack maps of Group 5 beams

CHAPTER V

5 SUMMARY AND CONCLUSIONS

5.1 CONCLUSIONS

This study aimed to investigate the behavior of reinforced concrete beams retrofitted by fiber reinforced ferrocement composites. Presented are the results of the mortar mixes studied as well as the reinforced concrete beams strengthened in flexure with fiber reinforced ferrocement laminates with different types and sizes of stirrups, fibers contents, number of mesh layers, thickness of laminate, and type of reinforcement.

The following conclusions are made:

- Partial replacement of Portland Cement by 5% Silica Fume greatly increases strength of mortar mix.
- Silica Fume reduces workability, which is why the addition of High range water reducing admixture is needed for a workable mortar mix. It is important for the mortar mix to be workable in cases of retrofitting in order to facilitate pumping.
- Fibers inclusion in the mortar mix at 0.1 to 0.2% content in volume does not affect workability and increases tensile strength of the mortar by up to 20%.
- Mortar mixes made with Portland cement are susceptible to very high drying shrinkage results, which is why the use of crack reducing admixture is crucial to limit shrinkage, which in terms limits cracking.
- Micro polypropylene fibers in the mortar mix do not increase tensile strength, but do reduce shrinkage significantly

- Steel fibers in mortar, increase the tensile strength but have no effect on shrinkage.
- Mortar with Macro fibers showed high tensile strength results and relatively low shrinkage result (less shrinkage than mortar with steel fibers)
- The use of Fiber reinforced Ferrocement in retrofitting beams that are deficient in flexure is effective in increasing the cracking load as well as the ultimate load, and improves ductility
- For a noticeable improvement in flexural behavior, a minimum of two mesh layers in the laminte is needed, when the thickness of the ferrocement layer is 1".
- Additional layers of mesh directly results in a higher cracking load, as well as higher ultimate load.
- The increase in the fibers percentages in the laminate, as well as the steel reinforcement demonstrated a significant improvement on the flexural behavior of the repaired Reinforced Concrete beam by delaying crack appearance giving higher ultimate load.
- The presence of macro fibers in the mortar mix used to fabricate the laminate delays cracking and reduces crack width
- Fibers without mesh in the laminate do not have a significant improvement on capacity of beams, and for that reason, we can conclude that fibers and at least two mesh layers are needed for a remarkable increase in strength and ductility
- The use of #3 studs resulted in a higher cracking load compared to the use of #2 studs. Furthermore, the size of shear connectors, (#2 or #3) did not affect the ultimate load.

5.2 SCOPE FOR FUTURE RESEARCH

This study focused on the use of three different fiber types for mortar reinforcement for the fabrication of the laminate repair layer at 0.1% and 0.2% in volume. Future studies on retroffitting concrete beams with fiber reinforced ferrocement can be done using a combination of two different fiber types. The effect of a higher percentage of fibers in the mortar mix can also be explored (0.3% to 0.5%).

In addition, this study focused on the effect of silica fume as a 5% replacement of portland cement. A higher percentage of silica fume can be evaluated as well as the effect of different cementitious materials used in the mortar mix such as slag or fly ash or multiple combination of different cementitious materials to replace portland cement.

REFERENCES

ACI Committee 549. (1997). *State-of-the-Art Report on Ferrocement: (ACI 549-97); and commentary (ACI 549R-97)*. Farmington Hills, MI: American Concrete Institute,

ACI Committee 116. (2000). Cement and Concrete Technology, manual of concrete practice, part 1: (ACI 116:00); and commentary (ACI 116R-00) Farmington Hills, MI: American Concrete Institute,

Antoni, Chandra, L., Hardjito, D. (2015). The impact of using fly ash, silica fume and calcium carbonate on the workability and compressive strength of mortar, *Procedia Engineering, 125*, 121-131.

ASTM International. (2013). *ASTM C0511-13: Standard Specification for Mixing Rooms, Moist Cabinets, Moist Rooms, and Water Storage Tanks Used in the Testing of Hydraulic Cements and Concretes.* Retrieved from http://dx.doi.org/10.1520/C0511-13.

ASTM International. (2014). *ASTM C305-14: Mechanical Mixing of Hydraulic Cement Pastes and Mortars of Plastic Consistency*. Retrieved from http://dx.doi.org/10.1520/C0305-14.

ASTM International. (2014). *ASTM C469/C469M–14: Standard Test Method for Static Modulus of Elasticity and Poisson's Ratio of Concrete in Compression.* Retrieved from http://dx.doi.org/10.1520/C469/C469M–14

ASTM International. (2014). *ASTM C469/C469M–14: Standard Test Method for Static Modulus of Elasticity and Poisson's Ratio of Concrete in Compression.* Retrieved from http://dx.doi.org/10.1520/C469/C469M–14

ASTM International. (2016). *ASTM C109/C109M-16a: Standard Test Method for Compressive Strength of Hydraulic Cement Mortars (Using 2-in. or [50-mm] Cube Specimens)*. Retrieved from http://dx.doi.org/10.1520/C0109_C0109M-16A

ASTM International. (2016). *ASTM C192/C192M − 16a: Standard Practice for Making and Curing Concrete Test Specimens in the Laboratory.* Retrieved from http://dx.doi.org/10.1520/C0192_C0192M-16A.

ASTM International. (2017). *ASTM C172/C172M–17: Standard Practice for Sampling Freshly Mixed Concrete.* Retrieved from http://dx.doi.org/10.1520/C0172_C0172M-17.

ASTM International. (2017). *C490/C490M – 17: Standard Practice for Use of Apparatus for the Determination of Length Change of Hardened Cement Paste, Mortar, and Concrete.* Retrieved from http://dx.doi.org/10.1520/C490/C490M−17

ASTM International. (2017). *ASTM C496/C496M–17: Standard Test Method for Splitting Tensile Strength of Cylindrical Concrete Specimens.* Retrieved from http://dx.doi.org/10.1520/C496/C496M–17

ASTM International. (2017). *ASTM C157/C157M–17: Standard Test Method for Length Change of Hardened Hydraulic-Cement Mortar and Concrete.* Retrieved from http://dx.doi.org/10.1520/C157/C157M–17

ASTM International. (2017). *ASTM C78/C78M−18: Standard Test Method for Flexural Strength of Concrete (Using Simple Beam with Third-Point Loading).* Retrieved from http://dx.doi.org/10.1520/ C78/C78M−18

ASTM International. (2018). *ASTM C39/C39M–18: Standard Test Method for Compressive Strength of Cylindrical Concrete Specimens.* Retrieved from http://dx.doi.org/10.1520/C39/C39M–18

Bruhwiler, E., & Denarie, E. (2013). Rehabilitation and strengthening of concrete structures using ultra-high performance fiber reinforced concrete. *Structural Engineering International*, *23*, 450-457.

Cairns, J., Plizzari, G.A., Du, Y., Law, D.W., & Franzoni, C. (2005). Mechanical properties of corrosion-damaged reinforcement, *American Concrete Institute Materials Journal, 102(4)*, 256–264.

Corrosion in Concrete. (n.d.). In *NASA, Kennedy Space Center, Corrosion Technology Laboratory.* Retreived from https://corrosion.ksc.nasa.gov/corrincon.htm

Federal Highway Administration. (2016). The State of The Nation's Highway and bridges, Condition and Performance and Highway Bridge Replacement and Rehabilitation Program, US Department of Transportation, Washington, DC.

Gheitasi, A., & Harris, D.K. (2015). Performance assessment of steel–concrete composite bridges with subsurface deck deterioration. *Structures, 2*, 8-20.

Hawileh, R.A., Abu-Obeidah, A., Abdalla, J.A., Al-Tamimi, A. (2015). Temperature effect on the mechanical properties of carbon, glass and carbon–glass FRP laminates. *Construction and Building Materials, 75,* 342-348.

Khan, S.U., Rafeeqi, S.F.A., & Ayub, T. (2013). Strengthening of RC Beams in Flexure using Ferrocement, *Iranian Journal of Science & Technology, Transactions of Civil Engineering, 37*, 353-365.

Makki, R.F. (2014). Response Of Reinforced Concrete Beams Retrofitted By Ferrocement, *International Journal Of Scientific & Technology Research, 3(9)*

Misra, S., & Uomoto, T. (1987). Effect of Corrosion of Reinforcement on the Load Carrying Capacity of RC Beam, Proceedings of Japan Concrete Institute Annual Conference, 9(2), 675–680.

Mousavi, S.E. (2017). Flexural response and crack development properties of ferrocement panels reinforced with steel fibers, *Journal of Building Engineering, 12,* 325-331.

Nassif, H.H., & Najm, H. (2004). Experimental and analytical investigation of ferrocement-concrete composite beams. *Cement & Concrete Composites*, *26*, 787-796.

Nowak, A.S., Nassif, H.H., & DeFrain, L. (1993). Effect of truck loading on girder bridges, *Journal of Transportation Engineering, 119*, 853-867.

Rodriguez, J., Ortega, L., & Casal, J., & Diez, J.M. (1996). Assessing Structural Conditions of Concrete Structures with Corroded Reinforcement, *Conference, Concrete Repair, Rehabilitation and Protection*, Dundee, 1996. (pp. 65–78). London: E. & F.N. Spon.

Rodriguez, J., Ortega, L., & Casal, J. (1997). Load carrying capacity of concrete structures with corroded reinforcement. *Construction Building Materials, 11*, 239–248.

Safdar, M., Matsumoto, T., & Kakuma, H. (2016). Flexural behavior of reinforced concrete beams repaired with ultra-high performance fiber reinforced concrete (UHPFRC). *Composite Structures*, *157*, 448-460.